1971

A triangular element for numerical solutions of axisymmetric conduction problems in cylindrical coordinates

Prafulla Chandra Mahata

Department:

A TRIANGULAR ELEMENT FOR NUMERICAL SOLUTIONS OF AXISYMMETRIC CONDUCTION PROBLEMS IN CYLINDRICAL COORDINATES

by

PRAFULLA CHANDRA MAHATA, 1947-

A

THESIS

Presented to the Faculty of the Graduate School of the

UNIVERSITY OF MISSOURI-ROLLA

In Partial Fulfillment of the Requirements for the Degree

MASTER OF SCIENCE IN MECHANICAL ENGINEERING

1971

Approved by

Orlo McMurry (Advisor) D C Cook Jr.

C A Johnson

ABSTRACT

The triangular element is one of the many suitable elements which are used in finite difference methods as applied to conduction heat transfer. Such elements find many applications in conduction problems in Cartesian coordinates. This work proposes a new triangular element for axisymmetric conduction problems in cylindrical coordinates. The validity and workability of the networks formed by the proposed triangular elements are strengthened by selected examples. The work is completed by the application of the triangular element to an industrial problem having irregular boundaries. The results are compared with the solution obtained by the finite element method.

ACKNOWLEDGEMENTS

The author wishes to extend sincere thanks and appreciation to his advisor, Dr. R.O. McNary, for the initial motivation and valuable suggestions, guidance and encouragement throughout the course of this thesis.

The author is grateful to Dr. R.L. Davis, Dr. H.D. Keith and Mr. K. Hambacker for providing the finite element solution in Chapter V, and to Dr. D.C. Look for his critical review of the work.

Thanks are due also to Mrs. Connie Hendrix for typing the thesis.

TABLE OF CONTENTS

Page

ABSTRACT ii

ACKNOWLEDGEMENTS iii

LIST OF ILLUSTRATIONS vi

LIST OF TABLES viii

LIST OF SYMBOLS ix

I. INTRODUCTION 1

II. DEVELOPMENT OF THE TRIANGULAR NETWORK . . . 10

A. Geometric Factors for a Rectangular Element 10

B. Geometric Factors for a Triangular Element 12

III. VALIDITY OF THE TRIANGULAR NETWORK IN CYLINDRICAL COORDINATES 16

A. Parameters in the Geometric Factor . . . 16

B. Deviation in the Geometric Factors for the Triangular Element 19

IV. COMPARISON OF SOLUTIONS USING THE PROPOSED TRIANGULAR ELEMENT WITH SOLUTIONS BY OTHER METHODS 33

A. An Infinitely Long Hollow Cylinder . . . 33

i. Analytical Method 34

ii. Rectangular Network Method 36

iii. Triangular Network Method 38

B. A Circular Fin With Rectangular Profile 45

i. Analytical Method 45

ii. Rectangular Network Method 48

iii. Triangular Network Method 50

TABLE OF CONTENTS (Continued)

Page

C. A Solid Cylinder of Finite Length . . . 56

i. Analytical Method 57

ii. Rectangular Network Method 60

iii. Triangular Network Method 61

V. AN INDUSTRIAL APPLICATION 66

VI. CONCLUSION. 76

BIBLIOGRAPHY 78

VITA 79

APPENDICES 80

A. LENGTHS OF PERPENDICULAR BISECTORS OF A TRIANGULAR ELEMENT IN CYLINDRICAL COORDINATE SYSTEM 80

B. AN ALGEBRAIC APPROACH TO RELATE THE THERMAL CONDUCTANCES OF RECTANGULAR AND TRIANGULAR ELEMENTS IN CYLINDRICAL COORDINATES 83

LIST OF ILLUSTRATIONS

Figure		Page
1	Rectangular Network Element	3
2	A Portion of a Rectangular Network in a Two Dimensional Rectangular Coordinate System	3
3	A Portion of a Triangular Network in a Two Dimensional Rectangular Coordinate System	3
4	Equivalence of Rectangular and Triangular Networks in Two Dimensional Rectangular Coordinates	5
5	One Quarter View of the Rectangular and Triangular Elements	11
6	A Section of the Rectangular and Triangular Elements	11
7	Rectangular and Triangular Elements in Cylindrical Coordinates	18
8	Comparison of Deviations in the Geometric Factors of the Three Cases for Triangular Elements	27
9	Comparison of Deviations in Geometric Factors for Rectangular and Triangular Elements	32
10	Rectangular and Triangular Networks With Three Nodes for an Annular Ring . . .	34
11	Rectangular and Triangular Networks With One Node	41
12	Rectangular and Triangular Networks With Two Nodes	41
13	Deviation in Heat Transfer Rates for Rectangular and Triangular Networks	43
14	Rectangular and Triangular Networks in a Circular Fin	46

LIST OF ILLUSTRATIONS (Continued)

Figure		Page
15	Temperature Distribution in a Circular Fin by Three Methods	55
16	Comparison of Deviations in Heat Transfer Rates for Rectangular and Triangular Network Methods	55
17	Rectangular and Triangular Networks in a Finite Solid Circular Cylinder	58
18	Temperature Distribution in a Solid Cylinder of Finite Length by Three Methods .	65
19	Deviations in the Dimensionless Temperatures by Two Methods for a Solid Cylinder of Finite Length	65
20	Section of the Bottom of a Reaction Vessel .	67
21	Use of the Triangular Network in an Irregular Weld Joint	69
A1	A Triangular Element in Two Dimensional Cylindrical Coordinates	80
B1	A Sectional View of the Rectangular and Triangular Elements	84

LIST OF TABLES

Table		Page
I	Percentage Deviations in Resultant Geometric Factors for Triangular Elements	25
II	Percentage Deviations in Geometric Factors for Rectangular and Triangular Elements. . .	31
III	Temperatures and Heat Transfer Rates for an Infinitely Long Hollow Cylinder Using Three Methods of Solution	42
IV	Temperatures and Heat Transfer Rates for a Circular Fin by Three Methods of Solution	54
V	Temperatures and Heat Transfer Rates for a Solid Cylinder by Three Methods of Solution	64
VI	Comparison of the Finite Difference and Finite Element Methods	72

LIST OF SYMBOLS

Q	heat transfer rate
k	conductivity
A	area of heat transfer
T	temperature
n	direction
S	geometric factor
K	thermal conductance
x,y	rectangular coordinates
r,z	cylindrical coordinates
Δ	increment
a,b,c,d,e,g,h,L	lengths
ε	percentage deviation
i	index of irregularity for one triangle
I	index of irregularity for a group of triangles
am	arithmetic mean
lm	logarithmic mean
r^*,z^*	dimensionless coordinates
d^*,e^*,L^*	dimensionless lengths
Q^*	dimensionless heat transfer rate
T^*	dimensionless temperature
h	convective heat transfer coefficient
λ^*	dimensionless eigenvalue
$\bar{r}$, ϕ	spherical coordinates
δ	percentage difference

I. INTRODUCTION

In many situations mathematical techniques are adequate to obtain analytical solutions of the problems encountered in many fields of Science and Engineering. However, in attacking irregular and complicated bodies, the mathematics may become extremely tedious. Cases are not rare wherein analytical solutions are impossible with the application of existing techniques. In such cases numerical methods are used successfully. Digital computers have added extra advantage and feasibility to the numerical methods in recent years. These methods have wide applicibility in the field of heat transfer by conduction in the calculation of the temperature distribution and heat transfer rates. Elements of several shapes such as rectangular, triangular, hexagonal and polar are commonly used in numerical methods. The present interest is in triangular elements which have the advantage of fitting into irregular geometries.

Elements are employed to give a finite difference form to the Fourier law of heat conduction which is stated as

$$Q = -kA \frac{\partial T}{\partial n}, \qquad (1)$$

where Q, k, A, T and n are the heat transfer rate, conductivity, area of heat transfer, temperature and direction

of heat transfer, respectively. Using the rectangular element (Fig. 1) for preliminary illustration, the finite difference form of Eq. (1) is given by

$$Q = -kA\ \Delta T/\Delta n, \tag{2}$$

where ΔT and Δn are incremental quantities. Related to the finite difference form of the law of conduction heat transfer are the geometric factor S and the thermal conductance K of the element, which are defined by [1]

$$S = A/\Delta n, \qquad K = kA/\Delta n, \tag{3}$$

respectively. Introducing Eqs. (3) into Eq. (2), results in

$$Q = -K\ \Delta T. \tag{4}$$

Recognizing Q as the current, 1/K as the resistance and ΔT as the potential difference, Eq. (4) is analogous to Ohm's law in electrical technology. This analogy leads to the possible network representation of any physical problem in conduction heat transfer. A network is defined to consist of heat conducting rods which represent the elements and which are connected to each other in a particular way depending on the type of the elements. The junctions are called nodes of the network. Before introducing the actual subject matter of the present work, some common types of networks and related facts are

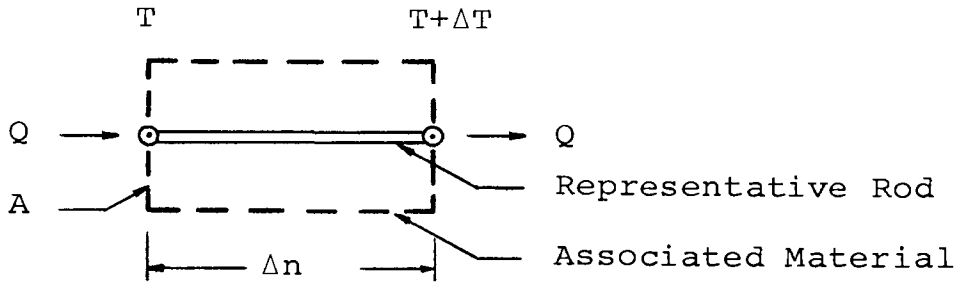

Fig. 1. Rectangular Network Element

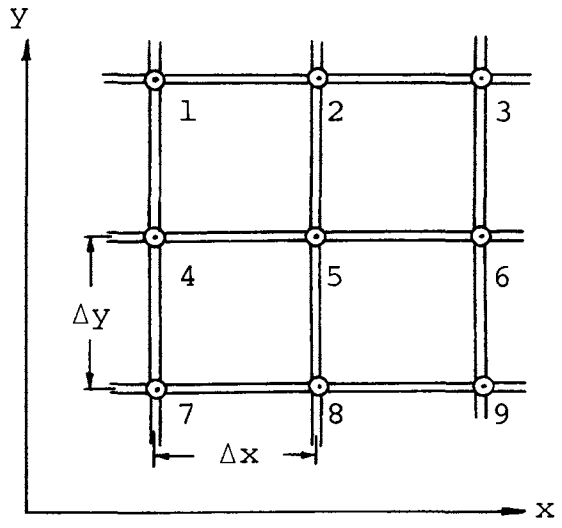

Fig. 2. A Portion of a Rectangular Network in a Two Dimensional Rectangular Coordinate System

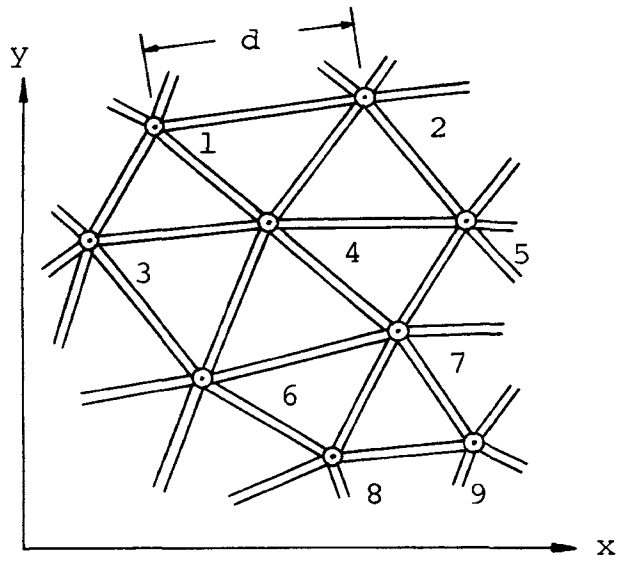

Fig. 3. A Portion of a Triangular Network in a Two Dimensional Rectangular Coordinate System

discussed to serve as ground work.

A. Common Networks

In two dimensional Cartesian coordinates the commonly used networks are rectangular (Fig. 2), triangular (Fig. 3), hexagonal, polar, etc.

It is known that the rectangular network solutions approach the analytical results, as the dimensions of the biggest element in the network approach zero ($\Delta x \to 0$, $\Delta y \to 0$). The triangular network involves multiple directions and variable areas of heat transfer (Fig. 3). It may be difficult to prove by the direct method of letting the elemental dimension approach zero that the triangular network solutions approach the analytical results. However, the validity of the triangular network has been established by Dusinberre[1] with the aid of an indirect method. A brief outline of this method is given here to link the present work with Dusinberre's. Dusinberre's analysis established the equivalence of rectangular and triangular networks in two dimensional rectangular coordinates by showing the equality of the thermal conductances of the elements of the two networks. Consequently, the validity of the triangular network has been proved.

The element AXYZ (Fig. 4) of a rectangular network in two dimensional rectangular coordinates is composed of the

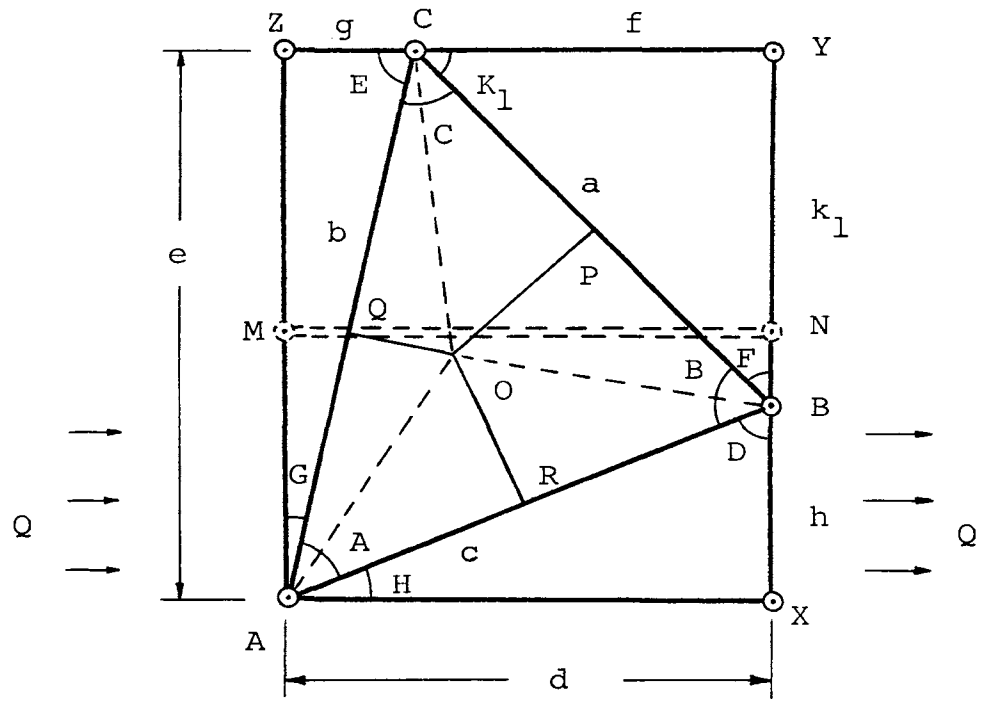

Fig. 4. Equivalence of Rectangular and Triangular Networks in Two Dimensional Rectangular Coordinates

elements ABC, AXB, BYC and CZA of a triangular network. The two main features are that

1. the angle H is arbitrary and
2. none of the triangular elements has obtuse angles so that the point of intersection of the perpendicular bisectors remains inside the element.

The geometric factor and the thermal conductance of the rectangular element AXYZ, which has unit depth, are given by

$$S_{M-N} = e/d \ , \quad K_{M-N} = k\ e/d. \tag{5}$$

The subscripts M-N imply from node M to node N; but to be physically consistent, it is necessary that $S_{M-N} = S_{N-M}$ and $K_{M-N} = K_{N-M}$. Dusinberre has defined the geometric factors of a triangular element (Fig. 4) as

$$S_{A-B} = OR/AB, \ S_{B-C} = OP/BC, \ S_{C-A} = OQ/CA, \tag{6}$$

which can be rephrased as

$$S_{A-B} = (\text{COT } C)/2, \ S_{B-C} = (\text{COT } A)/2, \quad S_{C-A} = (\text{COT } B)/2 \ . \tag{7}$$

In a similar manner, the geometric factors pertaining to the other elements in Fig. 4 are

$$S_{A-X} = (\text{COT } D)/2,\ S_{C-Y} = (\text{COT } F)/2,$$
$$S_{C-Z} = (\text{COT } G)/2. \tag{8}$$

By the electrical network analogy the total thermal conductance K_T of all the triangular elements in Fig. 4 is the resultant of the thermal conductances of the representative heat conducting rods ZC, AC, CY, CB, AB, AX and is given by

$$K_T = 1/[1/(k\ S_{C-A}+k\ S_{C-Z})+ 1/(k\ S_{B-C}+k\ S_{C-Y})] + k\ S_{A-B}+ k\ S_{A-X}, \tag{9}$$

which simplifies to

$$K_T = (k/2)[(\text{COT } A + \text{COT } F)(\text{COT } B + \text{COT } G)/(\text{COT } A + \text{COT } F + \text{COT } B + \text{COT } G) + \text{COT } C + \text{COT } D]. \tag{10}$$

Further simplification with the aid of trigonometric relations results in [1]

$$K_T = k\ e/d. \tag{11}$$

Comparison of Eqs. (5) and (11) shows that

$$K_{M-N} = K_T, \tag{12}$$

which proves that the triangular elements are equivalent to the rectangular element for arbitrarily chosen direction

of heat transfer (angle H being arbitrary) and with suitably defined geometric factors for the triangular elements.

The triangular network discussed so far is in two dimensional rectangular coordinates and thus it is applicable to plane bodies only. This limitation points out the need for a triangular network in two dimensional cylindrical coordinates (r,z), which can handle irregular axisymmetric bodies. Unfortunately, the work of Dusinberre in the rectangular coordinate system has not been extended to the cylindrical coordinate system.

Reid [2] determined analytically the steady state temperature distribution for the special case of a 30-degree right triangle with temperatures specified on the boundary. The solution is in two dimensional rectangular coordinates. The method is so involved that the author says, "To fully appreciate the difficulty involved, one should try to solve some other case such as a 31-degree right triangle."

Lancoz [3] and Garabedian [4] indicate that for irregular boundaries, the boundary value problem of even simple differential operators become practically unmanageable if the aim is to arrive at an analytical solution. The triangle in general form is an example of a region for which an explicit solution to the Dirichlet problem in closed form is presently unknown.

It appears that little work has been done on the triangular element in cylindrical coordinates. The present work provides a convenient and feasible definition of the geometric factors for the triangular network in two dimensional cylindrical coordinates (r,z). The validity of the network is established by proving that its accuracy is comparable to the rectangular network in cylindrical coordinates and that the accuracy improves as the size of the elements is decreased. Three examples further strengthen the reliability and the workability of such triangular networks. Another example of industrial interest is chosen to highlight all the major aspects of the application of the triangular network in two dimensional cylindrical coordinates.

II. DEVELOPMENT OF THE TRIANGULAR NETWORK

To develop the triangular network in two dimensional cylindrical coordinates (r,z), the prime task is to define the geometric factors of the triangular element in a suitable way. Three feasible definitions are given in this chapter and analysis using these definitions are considered. Before considering the triangular element, two alternate ways of defining geometric factors for a rectangular element in two dimensional cylindrical coordinates are discussed because of their use in succeeding chapters.

A. Geometric Factors for a Rectangular Element

The rectangular element with section AXYZ (Fig. 5), as shown in two dimensional cylindrical coordinates, forms a complete ring around the z-axis. Any radial plane intersecting the element forms a rectangular cross section.

On the basis of the arithmetic mean area, the geometric factor S_R of the rectangular element with section AXYZ (Fig.6) is defined as

$$S_R = \pi e(r_i + r_o)/(r_o - r_i), \tag{13}$$

where r_i, r_o and e are the internal and the external radii and the length of the element, respectively.

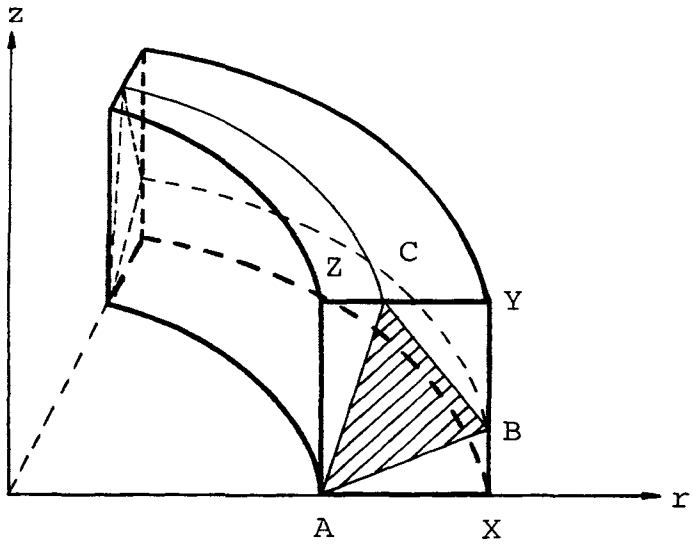

Fig. 5. One Quarter View of the Rectangular and Triangular Elements

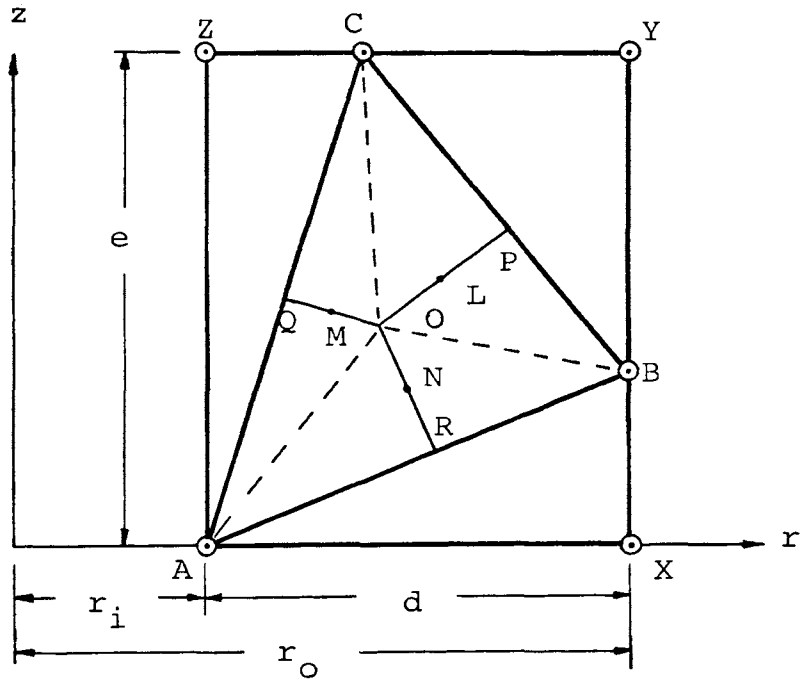

Fig. 6. A Section of the Rectangular and Triangular Elements

Introducing

$$d = r_o - r_i \tag{14}$$

in Eq. (13), yields

$$S_R = \pi e(2r_i + d)/d. \tag{15}$$

On the basis of the logarithmic mean area, the geometric factor S_R of the rectangular element is defined as [5]

$$S_R = 2\pi e/\ln(r_o/r_i). \tag{16}$$

B. Geometric Factors for a Triangular Element

The triangular element with section ABC (Fig.5) is a ring around the z-axis and results in a triangular cross section with the intersection of any radial plane. The perpendicular bisectors OP, OQ and OR intersect at a common point O inside the element as shown in Fig. 6. The geometric factors for triangular element ABC can be written in a manner similar to Eqs. (6) as

$$S_{A-B} = (\text{Area of surface of revolution by OR})/AB,$$

$$S_{B-C} = (\text{Area of surface of revolution by OP})/BC, \tag{17}$$

$$S_{C-A} = (\text{Area of surface of revolution by OQ})/CA.$$

The areas of surfaces of revolutions by OR, OP and OQ are considered in three different possible ways, which give rise to three possible definitions for the geometric factors.

Case 1: Areas Based on Mid-Radii of Perpendicular Bisectors

In this case the areas across OR, OP and OQ are the exact areas of the cylindrical surfaces containing OR, OP and OQ. So Eqs. (17) give

$$S_{A-B} = 2\pi[(r_O+r_R)/(2AB)]OR,\ S_{B-C} = 2\pi[(r_O+r_P)/(2BC)]OP,$$
$$S_{C-A} = 2\pi[(r_O+r_Q)/(2CA)]OQ, \tag{18}$$

where the subscript of the radius r implies radius to that point.

Case 2: Areas Based on Common Radius of Perpendicular Bisectors

In this case the areas of heat transfer are based on the radius corresponding to the common point O of the perpendicular bisectors. The geometric factors for the triangular elements are then obtained from Eqs. (17) as

$$S_{A-B} = 2\pi(r_O/AB)OR,\ S_{B-C} = 2\pi(r_O/BC)OP,$$
$$S_{C-A} = 2\pi(r_O/CA)OQ. \tag{19}$$

Case 3: Areas Based on Mid-Radii of Conducting Rods

Considering the areas across the perpendicular bisectors based on the mid-radius of each side, the geometric factors for the triangular element are obtained from Eq. (17) as

$$S_{A-B} = 2\pi(r_R/AB)OR,\ S_{B-C} = 2\pi(r_P/BC)OP,\ S_{C-A}=2\pi(r_Q/CA)OQ. \tag{20}$$

It is noted that although the exact area is employed in case 1, the definition of the geometric factors are not unique. Thus it is required to consider the equivalence of the rectangular and the triangular elements in a two dimensional cylindrical coordinate system, as is exhibited in the case of the rectangular coordinate system in Eq. (12). Using the definitions of the geometric factors in case 1, an analysis of the equivalence of the rectangular and the triangular elements is given in Appendix B. The results of the analysis show that the exact equivalence does not exist in the cylindrical coordinate system. Any possibility of equivalence, considering case 2 and case 3, is discussed later. However, the exact equivalence of the two networks is not required. For example, the network of rectangular elements based on two different definitions of the geometric factors,

the arithmetic mean area and the log mean area, are non-equivalent. However, they are both used for general engineering practice.

The immediate task is then to analyze the deviations in the three definitions of the geometric factor for the triangular element as compared to the geometric factor for the rectangular element based on either the arithmetic mean area or the logarithmic mean area.

III. VALIDITY OF THE TRIANGULAR NETWORK IN CYLINDRICAL COORDINATES

The geometric factors and hence the thermal conductances are the basic parameters which govern the temperature distribution and the heat transfer rates obtained by the finite difference method. Thus any inaccuracy associated with the geometric factor causes errors in the temperature distribution and heat transfer rates. In this chapter the deviation in the geometric factor for the triangular element with respect to the geometric factor for the rectangular element is analyzed for all the cases (cases 1,2 and 3). The geometric factor for the rectangular element based on the arithmetic mean area is taken as the basis of comparison for convenience. However, a simple relation can be used to alter the basis for comparison. In order to consider the geometric factor for a triangular element, it is essential to specify the shape of the element. This shape is a major factor in the possible variation of the geometric factor.

A. Parameters in the Geometric Factor

Fig. 7 illustrates a rectangular element with section AXYZ in cylindrical coordinates, which is composed of triangular elements with sections ABC, AXB, BYC and CZA.

The perpendicular bisectors and the necessary dimensions are shown in the figure. The shape and location of the triangular element can be completely specified by the parameters r_i, d, e, g and h. Dividing these by r_i, the dimensionless parameters are obtained as

$$r_i^* = r_i/r_i = 1, \quad d^* = d/r_i, \; e^* = e/r_i, \; g^* = g/r_i, \; h^* = h/r_i. \tag{21}$$

The dimensionless parameter d* is taken as the measure of the size of the rectangular element and representative of the size of the triangular elements. However, the shapes of the triangular elements are dictated by all the four parameters d*, e*, g* and h*. A single index is introduced here to represent all possible shapes of the triangular element and to give an indication of the irregularity. Such an index of a triangle can be defined as the sum of the absolute values of the three differences of the angles in that triangle. Thus the value of the index i ranges from 0 to π as the irregularity of a triangle increases with the restriction of no obtuse angles. Another index I for a group of triangles may be defined as the sum of the individual indices of all the triangles in that group. The expression for I is given by

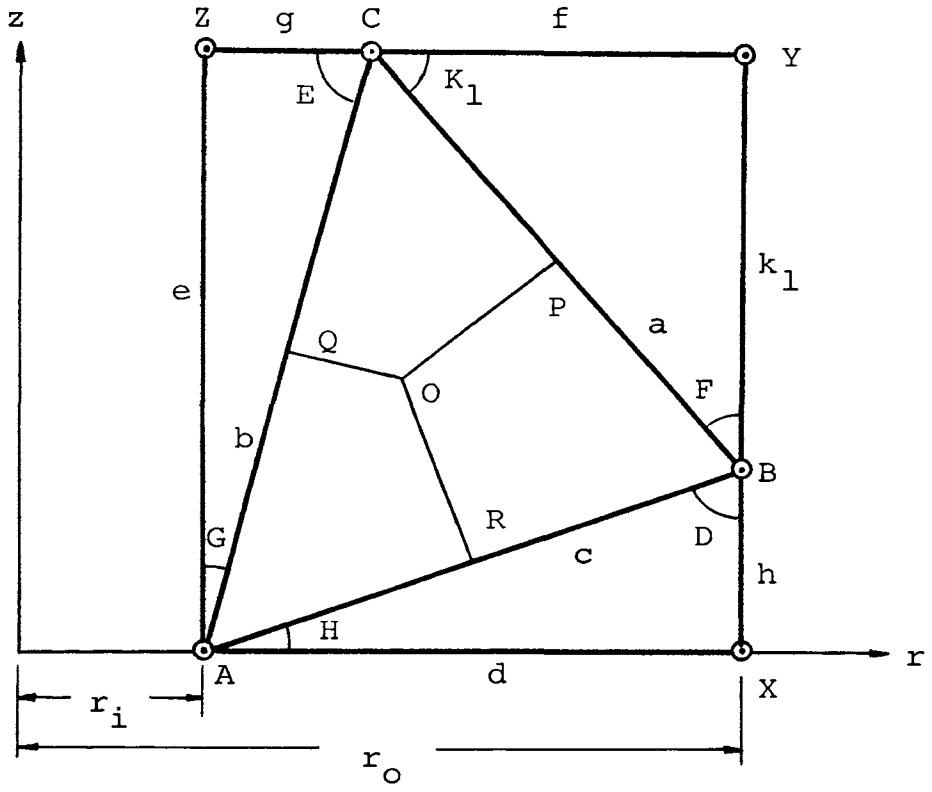

Fig. 7. Rectangular and Triangular Elements in Cylindrical Coordinates

$$I = |\angle A - \angle B| + |\angle B - \angle C| + |\angle C - \angle A|$$
$$+ |\angle H - \pi/2| + |\pi/2 - \angle D| + |\angle D - \angle H|$$
$$+ |\angle F - \pi/2| + |\pi/2 - \angle K_1| + |\angle K_1 - \angle F|$$
$$+ |\angle E - \pi/2| + |\pi/2 - \angle G| + |\angle G - \angle E|. \qquad (22)$$

Some of the quantities used in the definitions of the geometric factors for the triangular element are expressed here in dimensionless form in terms of the four

dimensionless independent parameters d*, e*, g* and h* as follows:

$$\angle F = \arctan[(d^*-g^*)/(e^*-h^*)],$$

$$\angle K_1 = \pi/2 - \angle F, \qquad \angle G = \arctan(g^*/e^*),$$

$$\angle E = \pi/2 - \angle G, \qquad \angle H = \arctan(h^*/d^*),$$

$$\angle D = \pi/2 - \angle H, \qquad \angle A = \pi/2 - (\angle H + \angle G),$$

$$b^* = g^*/\sin G, \qquad c^* = h^*/\sin H,$$

$$a^* = (b^{*2}+c^{*2}-2b^*c^*\cos A)^{1/2},$$

$$\angle B = \arcsin(b^*\sin A/a^*), \qquad \angle C = \arcsin(c^*\sin A/a^*),$$

$$OR^* = (c^*/2)\cot C,\ OP^* = (a^*/2)\cot A,\ OQ^* = (b^*/2)\cot B,$$

$$r_O^* = r_i^* + (c^*/2)\sin(C-H)/\sin C,$$

$$r_R^* = r_i^* + d^*/2, \qquad r_P^* = r_i^* + d^*/2 + g^*/2,$$

$$r_Q^* = r_i^* + g^*/2. \tag{23}$$

The geometric factor S_R for the rectangular element with section AXYZ based on the arithmetic mean area method, as given in Eq. (15), can be expressed in dimensionless form as

$$S_R^* = \pi e^*(2r_i^* + d^*)/d^*, \tag{24}$$

where

$$S_R^* = S_R/r_i. \tag{25}$$

B. Deviation in the Geometric Factors for the Triangular Element

In this section a comparison is made between the geometric factors for the triangular element and the geometric factor for the rectangular element defined on the basis of the arithmetic mean area. The three cases for the definition of the geometric factors, as discussed in the last chapter, will now be considered.

Case 1: Areas Based on Mid-Radii of Perpendicular Bisectors

In this case the geometric factors for the triangular element with section ABC obtained from Eqs.(18) with the aid of the trigonometric relations in Appendix B can be written in dimensionless forms as

$$S^*_{A-B} = \pi(\text{COT } C)(r_O^* + r_R^*)/2,$$

$$S^*_{B-C} = \pi(\text{COT } A)(r_O^* + r_P^*)/2,$$

$$S^*_{C-A} = \pi(\text{COT } B)(r_O^* + r_Q^*)/2. \qquad (26)$$

The dimensionless expressions for the necessary geometric factors for the other triangular elements in Fig. 7 are

$$S^*_{A-X} = \pi(\text{COT } D)r_R^*, \quad S^*_{C-Y} = \pi(\text{COT } F)r_P^*,$$

$$S_{C-Z} = \pi(\text{COT } G)r_Q^*. \qquad (27)$$

The dimensionless resultant thermal conductance of the triangular elements is obtained from Eq. (9) as

$$K_T^* = k^*[(S^*_{C-A} + S^*_{C-Z})(S^*_{B-C} + S^*_{C-Y})/(S^*_{C-A} + S^*_{C-Z} + S^*_{B-C} + S^*_{C-Y}) + S^*_{A-B} + S^*_{A-X}], \tag{28}$$

where

$$K_T^* = K_T/(k_o r_i),$$
$$k^* = k/k_o. \tag{29}$$

Symbol k_o denotes any reference thermal conductivity. The dimensionless resultant geometric factor obtained from Eq. (28) is

$$S_T^* = (S^*_{C-A} + S^*_{C-Z})(S^*_{B-C} + S^*_{C-Y})/(S^*_{C-A} + S^*_{C-Z} + S^*_{B-C} + S^*_{C-Y}) + S^*_{A-B} + S^*_{A-X}. \tag{30}$$

The percentage deviation ε_{tl} in the dimensionless resultant geometric factor for the triangular elements is

$$\varepsilon_{tl} = [(S_T^* - S_R^*)/S_R^*]100, \tag{31}$$

where S_R^* and S_T^* are given by Eqs. (24) and (30), respectively. It is noted that the individual dimensionless geometric factors and hence the dimensionless resultant geometric factor can be expressed solely in terms of d*, e*, g* and h* by the use of Eqs. (23).

Case 2: Area Based on Common Radius of the Perpendicular Bisectors

With reference to Eq. (19) and in a manner similar to case 1, the dimensionless form of the geometric factors are

$$\begin{aligned} S^*_{A-B} &= \pi(\text{COT C})r_O^*, & S^*_{A-X} &= \pi(\text{COT D})r_R^*, \\ S^*_{B-C} &= \pi(\text{COT A})r_O^*, & S^*_{C-Y} &= \pi(\text{COT F})r_P^*, \\ S^*_{C-A} &= \pi(\text{COT B})r_O^*, & S^*_{C-Z} &= \pi(\text{COT G})r_Q^*. \end{aligned} \tag{32}$$

The dimensionless resultant geometric factor is given by Eq. (30) with the values of the individual dimensionless geometric factors from Eqs. (32). The percentage deviation ε_{t2} is expressed in the same way as in case 1.

Case 3: Areas Based on the Mid-Radii of the Conducting Rods

In a manner similar to the last two cases, the dimensionless forms of the geometric factors, as obtained from Eq. (20), are

$$\begin{aligned} S^*_{A-B} &= \pi(\text{COT C})r_R^*, & S^*_{A-X} &= \pi(\text{COT D})r_R^*, \\ S^*_{B-C} &= \pi(\text{COT A})r_p^*, & S^*_{C-Y} &= \pi(\text{COT F})r_P^*, \\ S^*_{C-A} &= \pi(\text{COT B})r_Q^*, & S^*_{C-Z} &= \pi(\text{COT G})r_Q^*. \end{aligned} \tag{33}$$

Eq. (30) with the aid of Eqs. (33) gives the dimensionless resultant geometric factor. The percentage deviation ε_{t3} is again defined in the same manner as in the last two cases.

The following method was employed in order to compute the percentage deviations in the three cases for various shapes of the triangular elements.

a. Ten suitable values (0.04, 0.08,..., 0.40) of d* were chosen to represent the size of the triangular elements.

b. For each value of d*, ten suitable values (0.04, 0.08,...,0.40) of e* were used. These values alter the shape of the rectangular and the triangular elements.

c. For every value of e*, nine values of g* were taken at intervals of one-tenth of d*. For each value of g* nine values of h* were also considered at an interval of one-tenth of e*.

The total number of shapes considered by the above method is 8100. The shapes having obtuse angle were omitted for the reason previously stated. Table I lists the results of the computation giving the percentage deviations in all the three cases corresponding to a few particular shapes of the triangular elements. From the results of all possible shapes under study, it is observed that the case 3 gives the least percentage deviation for most of the considered shapes of the triangular elements. The list in Table I includes only those sets which have

Table I. Percentage Deviations in Resultant Geometric Factors for Triangular Elements

d*	e*	g*	h*	I	ε_{t1}	ε_{t2}	ε_{t3}
0.04	0.04	0.004	0.004	9.999	-0.046	-0.090	-0.002
	0.04	0.020	0.008	7.585	-0.083	-0.160	-0.006
	0.12	0.004	0.108	11.082	-0.398	-0.794	-0.002
	0.04	0.016	0.004	8.709	-0.049	-0.092	-0.006
0.08	0.08	0.008	0.016	9.530	-0.160	-0.313	-0.007
	0.08	0.040	0.016	7.585	-0.170	-0.320	-0.022
	0.24	0.008	0.216	11.082	-0.781	-1.558	-0.007
	0.04	0.024	0.004	10.081	-0.038	-0.051	-0.029
0.12	0.08	0.108	0.024	9.566	-0.142	-0.271	-0.014
	0.12	0.060	0.024	7.585	-0.262	-0.479	-0.048
	0.04	0.012	0.004	11.146	-0.030	-0.036	-0.027
	0.08	0.060	0.008	8.960	-0.097	-0.137	-0.062
0.16	0.16	0.144	0.144	9.317	-0.175	-0.334	-0.024
	0.16	0.080	0.032	7.585	-0.358	-0.637	-0.082
	0.40	0.064	0.360	10.847	-1.064	-2.085	-0.067
	0.08	0.048	0.008	10.081	-0.105	-0.113	-0.109
0.20	0.12	0.180	0.048	9.602	-0.219	-0.405	-0.036
	0.16	0.120	0.016	7.570	-0.225	-0.326	-0.131
	0.08	0.020	0.032	10.889	-0.128	-0.198	-0.063
	0.12	0.100	0.036	9.417	-0.271	-0.388	-0.175
0.24	0.24	0.216	0.024	9.182	-0.284	-0.521	-0.048
	0.24	0.120	0.048	7.585	-0.558	-0.950	-0.171
	0.08	0.024	0.008	11.146	-0.087	-0.083	-0.102
	0.12	0.072	0.012	10.081	-0.194	-0.184	-0.231

Table I (continued)

d*	e*	g*	h*	I	ε_{t1}	ε_{t2}	ε_{t3}
0.28	0.28	0.252	0.028	9.181	-0.332	-0.603	-0.062
	0.28	0.140	0.056	7.585	-0.661	-1.105	-0.224
	0.12	0.028	0.060	10.787	-0.215	-0.326	-0.112
	0.16	0.140	0.016	9.263	-0.287	-0.277	-0.332
0.32	0.24	0.288	0.048	9.425	-0.374	-0.671	-0.079
	0.28	0.160	0.028	7.337	-0.469	-0.640	-0.308
	0.12	0.032	0.036	10.983	-0.199	-0.256	-0.158
	0.16	0.096	0.016	10.081	-0.301	-0.261	-0.389
0.36	0.28	0.324	0.056	9.387	-0.446	-0.799	-0.094
	0.32	0.180	0.032	7.368	-0.553	-0.745	-0.374
	0.12	0.036	0.012	11.146	-0.163	-0.137	-0.216
	0.20	0.180	0.020	9.320	-0.412	-0.358	-0.525
0.40	0.40	0.360	0.040	9.181	-0.475	-0.840	-0.111
	0.36	0.200	0.036	7.392	-0.640	-0.852	-0.444
	0.16	0.040	0.064	10.889	-0.303	-0.401	-0.225
	0.24	0.200	0.072	9.417	-0.648	-0.779	-0.588

the minimum and the maximum percentage deviations in the preferred case 3 and the minimum and the maximum values of the index I. All the extreme values are underlined. The percentage deviations in the numerous other shapes are not listed mainly due to the unpredictable nature of the percentage deviations in terms of the index I and because of space limitations. However, Fig. 8 is used to represent all the results of the computation in the form of regions of percentage deviations corresponding to the representative size d* of the triangular element.

The results in Table I and Fig. 8 indicate the following:

1. The resultant geometric factor for the triangular elements approaches the geometric factor for the rectangular element as the size of the elements of the network decreases. This establishes the validity of the triangular network.

2. There is no preferred shape of the triangular elements.

3. The geometric factors formulated in the case 3 yield better results. It is noted that case 1 based on exact areas does not give the most accurate results. Thus case 3 is preferred

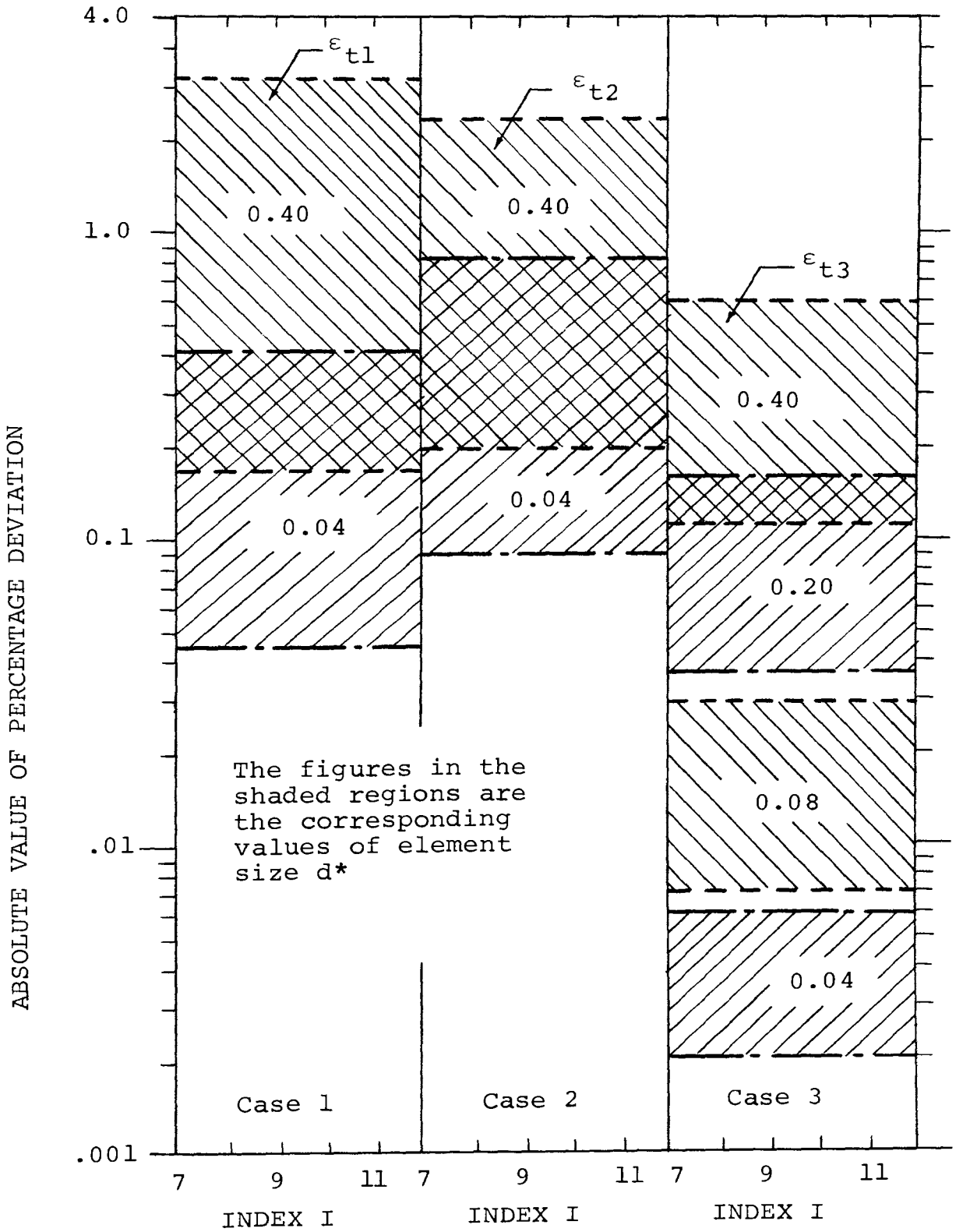

Fig. 8. Comparison of Deviations in The Geometric Factors of the Three Cases for Triangular Elements

for further use in triangular networks. Case 3 gives a rapid decrease in the percentage deviations in the resultant geometric factor with a decrease in d*. This is evident in Fig. 8. Also this formulation of the geometric factors is the simplest among the three cases under consideration.

The percentage deviation in the resultant geometric factor for the triangular elements (considering case 3) with respect to the geometric factor for the rectangular element based on the logarithmic mean area will now be analyzed for comparison. This analysis was done indirectly by the following methods.

From Eq. (15) the dimensionless geometric factor $S^*_{R_{am}}$ for the rectangular element based on the arithmetic mean area is given by

$$S^*_{R_{am}} = \pi e^*(2r^*_i + d^*)/d^*, \tag{34}$$

and from Eq. (16) the dimensionless geometric factor $S^*_{R_{lm}}$ based on the logarithmic mean area is

$$S^*_{R_{lm}} = 2\pi e^*/\ln[(r^*_i + d^*)/r^*_i]. \tag{35}$$

The percentage deviation ε_{am} in the geometric factor based on the arithmetic mean area with respect to that based on the logarithmic mean area is given by

$$\varepsilon_{am} = [(S^*_{R_{am}} - S^*_{R_{lm}})/S^*_{R_{lm}}]100, \quad (36)$$

which, combined with Eqs. (34) and (35), reduces to

$$\varepsilon_{am} = [(1/2 + 1/d^*)\ln(1 + d^*) - 1]100. \quad (37)$$

The case 3 version of Eq. (31) gives the percentage deviation ε_{t3} in the dimensionless resultant geometric factor for the triangular elements with respect to the geometric factor for the rectangular element based on the arithmetic mean area. The rearranged form of the above mentioned equation is

$$\varepsilon_{t3}/100 = S^*_T/S^*_{R_{am}} - 1. \quad (38)$$

Eq. (36) is rephrased as

$$\varepsilon_{am}/100 = S^*_{R_{am}}/S^*_{R_{lm}} - 1. \quad (39)$$

The percentage deviation ε_t in the resultant geometric factor for the triangular elements (considering case 3) with respect to the geometric factor for the rectangular element using the logarithmic mean area method is given by

$$\varepsilon_t = [(S^*_T - S^*_{R_{lm}})/S^*_{R_{lm}}]100, \quad (40)$$

which is rearranged as

$$\varepsilon_t = [S_T^*/S_{R_{lm}}^* - 1]100. \tag{41}$$

Eqs. (38) and (39) jointly give

$$S_T^*/S_{R_{lm}}^* = (\varepsilon_{t3}/100 + 1)(\varepsilon_{am}/100 + 1), \tag{42}$$

which, when introduced into Eq. (41), yields

$$\varepsilon_t = \varepsilon_{t3} + \varepsilon_{am}. \tag{43}$$

Using Table I, the minimum and the maximum values of ε_t were computed and result listed in Table II. Fig. 9 shows the variations of ε_{am} and ε_t versus the element size d*. It illustrates the following important facts.

1. ε_t is smaller than ε_{am} everywhere within the range of d* under consideration and for all of the 8100 shapes. Corresponding to d* = 0.40, the maximum values of ε_{am} and ε_t are 0.942 and 0.831 percent, respectively. As these deviations are comparable, the workability of the triangular network using formulations of case 3 may be assumed.

2. Both the minimum and the maximum values of ε_t decrease rapidly with a decrease in the size (d*) of the element. This indicates that the deviation approaches zero as the element size decreases.

Table II. Percentage Deviations in Geometric Factors for Rectangular and Triangular Elements

d*	ε_{am}	ε_t	
		minimum	maximum
0.04	0.013	0.007	0.011
0.08	0.049	0.020	0.042
0.12	0.107	0.045	0.093
0.16	0.183	0.074	0.159
0.20	0.277	0.102	0.241
0.24	0.385	0.154	0.337
0.28	0.507	0.175	0.445
0.32	0.642	0.253	0.563
0.36	0.787	0.262	0.693
0.40	0.942	0.364	0.831

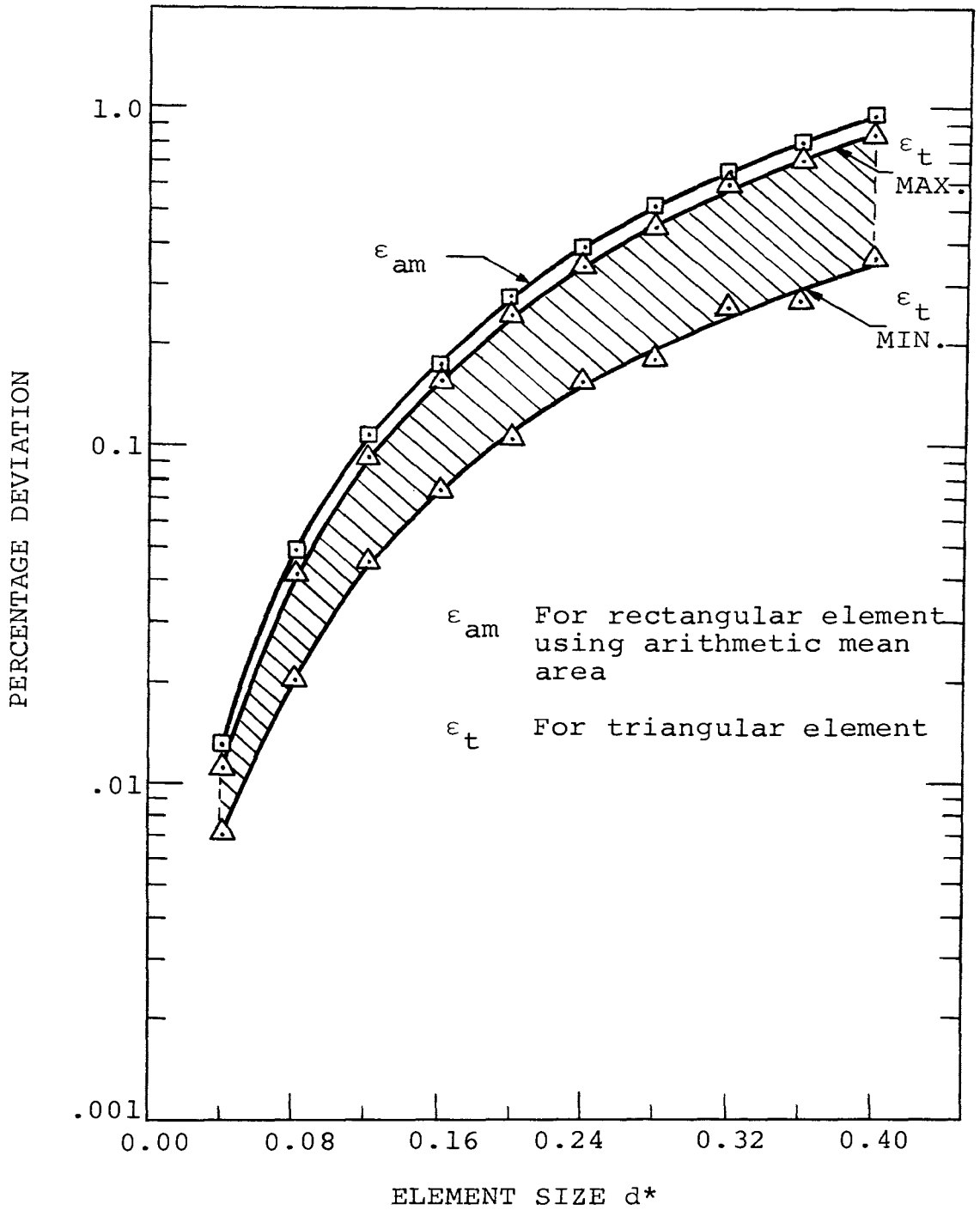

Fig. 9. Comparison of Deviations in Geometric Factors for Rectangular and Triangular Elements

IV . COMPARISON OF SOLUTIONS USING THE PROPOSED TRIANGULAR ELEMENT WITH SOLUTIONS BY OTHER METHODS

Since case 3 is the preferred formulation, henceforth all the triangular networks are based on that formulation. Three examples have been selected to illustrate the workability of the triangular network by comparison with the rectangular network (arithmetic mean area method) and with analytical methods. An equal number of nodes are employed wherever possible in both the rectangular and the triangular network methods to obtain fair comparison. For convenience in the analysis, steady state conduction problems with constant thermal conductivity for the case of no heat sources or sinks will be considered. These complicating factors may be treated by the usual methods.

The first example in the series will now be illustrated using the three different methods.

A. An Infinitely Long Hollow Cylinder

Fig. 10 shows a cross section of an annular ring which is a part of an infinitely long hollow cylinder. This will be treated as a one dimensional problem. Using the constants T_i and T_o as the inside and the outside temperatures, the purpose now is to find the

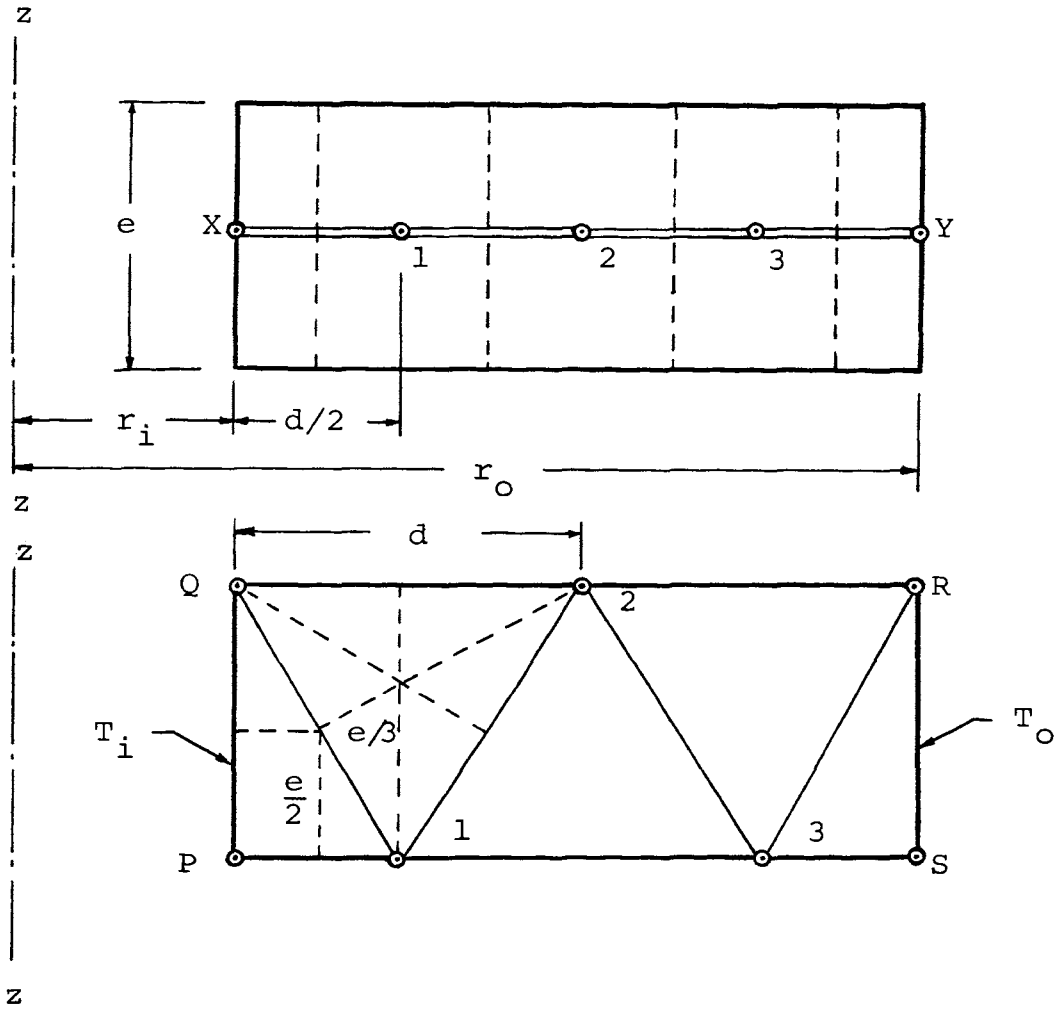

Fig. 10. Rectangular and Triangular Networks with Three Nodes for an Annular Ring

temperature distribution and the heat transfer rate by the analytical method, by the rectangular network method and by the triangular network method.

i. Analytical Method

The differential equation governing the heat conduction is given by

$$\frac{d}{dr}\left(r\frac{dT_a}{dr}\right) = 0, \tag{44}$$

where the subscript a denotes the analytical method. The boundary conditions are

$$T_a(r_i) = T_i, \qquad T_a(r_o) = T_o. \tag{45}$$

The dimensionless temperature T_a^* and heat transfer rate Q_a^* per unit length are given as

$$T_a^* = 1 - \ln r^*/\ln r_o^*, \tag{46}$$

$$Q_a^* = (T_i^* - T_o^*)/[(1/2\pi)\ln(1 + d^*)], \tag{47}$$

where the dimensionless quantities are defined by

$$\begin{aligned}
&T_a^* = (T_a-T_o)/(T_i-T_o), \quad T_i^* = (T_i-T_o)/(T_i-T_o),\\
&T_o^* = (T_o-T_o)/(T_i-T_o)\\
&Q_a^* = Q_a/[r_i ke^*(T_i-T_o)],\\
&r^* = r/r_i, \qquad r_o^* = r_o/r_i,\\
&d^* = [(r_o-r_i)/2]/r_i,\\
&e^* = \sqrt{3}\, d^*/2.
\end{aligned} \tag{48}$$

Noting that $r_o^* = 1 + 2d^*$, $T_i^* = 1$ and $T_o^* = 0$, the dimensionless temperatures T_{a1}^*, T_{a2}^*, etc., and the heat transfer rate per unit length are computed from Eqs.(46)

and (47) corresponding to the values of d* and r*. The results are given in Table III,page 42.

ii. Rectangular Network Method

A rectangular network is formed for the annular ring as shown in Fig. 10 and an energy balance is performed at each of the three nodes to obtain

$$\begin{aligned} K_{X-1}(T_i^* - T_1^*) + K_{2-1}(T_2^* - T_1^*) &= 0, \\ K_{1-2}(T_1^* - T_2^*) + K_{3-2}(T_3^* - T_2^*) &= 0, \\ K_{2-3}(T_2^* - T_3^*) + K_{Y-3}(T_o^* - T_3^*) &= 0. \end{aligned} \tag{49}$$

The thermal conductances for the rectangular elements by the arithmetic mean area method are

$$\begin{aligned} K_{X-1} &= k\ 2\pi e(r_i + d/4)/(d/2), \\ K_{1-2} &= k\ 2\pi e(r_i + 3\ d/4)/(d/2), \\ K_{2-3} &= k\ 2\pi e(r_1 + 5\ d/4)/(d/2), \\ K_{3-Y} &= k\ 2\pi e(r_i + 7\ d/4)/(d/2). \end{aligned} \tag{50}$$

Inserting the values of the thermal conductances from Eqs. (50) in Eqs. (49), solving for the dimensionless temperatures and dividing numerator and denominator by r_i, yield

$$T_1^* = [(1+d^*/4)T_i^* + (1+3d^*/4)T_2^*]/(2+d^*),$$

$$T_2^* = [(1+3d^*/4)T_1^*+(1+5d^*/4)T_3^*]/(2+2d^*), \qquad (51)$$

$$T_3^* = [(1+5d^*/4)T_2^*+(1+7d^*/4)T_o^*]/(2+3d^*).$$

The above set of equations was solved for the dimensionless temperatures using the Gauss-Seidel iterative method [6] with suitable values of d*. The iteration process was terminated when the maximum difference in the values of any of the unknown temperatures, obtained by the successive iterations, was 0.5×10^{-6}. The heat transfer rate in per unit length at the interior surface can be expressed as

$$Q = K_{X-1}(T_i - T_1)/e. \qquad (52)$$

Introducing K_{X-1} from Eqs. (50) in Eq. (52) and non-dimensionalizing, yields

$$Q^* = 2\pi[(1 + d^*/4)/(d^*/2)](T_i^* - T_1^*). \qquad (53)$$

In a similar manner the expression for heat transfer rate at the outer surface can be obtained. The percentage deviation ε_1 in the temperature at node 1 with respect to the analytical case based on the maximum temperature range is given in dimensionless form as

$$\varepsilon_1 = (T_1^* - T_{a1}^*)100. \qquad (54)$$

Similar expressions are used to find ε_2 and ε_3 corresponding to node 2 and node 3, respectively. The percentage deviation ε_q in the heat transfer rates with respect to the analytical method takes the dimensionless form

$$\varepsilon_q = [Q^* - Q_a^*)/Q_a^*]100. \tag{55}$$

The nodal dimensionless temperatures with the corresponding percentage deviations and the heat transfer rates with the corresponding percentage deviations are listed in Table III.

iii. Triangular Network Method

A triangular network is shown in Fig. 10. For convenience in analysis, as many regular triangular elements as possible are used. The nodes are located at the same radial positions as in the rectangular network. An energy balance at each node in terms of the dimensionless temperatures is performed to obtain

$$\begin{aligned}
&K_{P-1}(T_i^* - T_1^*) + K_{Q-1}(T_i^* - T_1^*) + K_{2-1}(T_2^*-T_1^*)+K_{3-1}\\
&\quad (T_3^* - T_1^*) = 0,\\
&K_{1-2}(T_1^* - T_2^*) + K_{Q-2}(T_i^* - T_2^*) + K_{R-2}(T_o^* - T_2^*) +\\
&\quad K_{3-2}(T_3^* - T_2^*) = 0,\\
&K_{1-3}(T_1^* - T_3^*) + K_{2-3}(T_2^* - T_3^*) + K_{R-3}(T_o^* - T_3^*) +\\
&\quad K_{S-3}(T_o^* - T_3^*) = 0,
\end{aligned} \tag{56}$$

where the thermal conductances are given by

$$K_{P-1} = k2\pi(r_i+d/4)(e/2)/(d/2),$$

$$K_{Q-1} = k2\pi(r_i+d/4)(e/3)/d, \quad K_{2-1} = k2\pi(r_i+3d/4)(2e/3)/d,$$

$$K_{3-1} = k2\pi(r_i+d)(e/3)/d, \quad K_{Q-2} = k2\pi(r_i+d/2)(e/3)/d,$$

$$K_{R-2} = k2\pi(r_i+3d/2)(e/3)/d, \quad K_{3-2} = k2\pi(r_i+5d/4)(2e/3)/d,$$

$$K_{R-3} = k2\pi(r_i+7d/4)(e/3)/d, \quad K_{S-3} = k2\pi(r_i+7d/4)(e/2)/(d/2). \tag{57}$$

Introducing the values of the thermal conductances into Eqs. (56) and solving for the dimensionless nodal temperatures, yield

$$T_1^* = [3(1 + d^*/4)T_i^* + (1 + d^*/4)T_i^* + 2(1 + 3d^*/4)T_2^* + (1 + d^*)T_3^*]/(7 + 7d^*/2),$$

$$T_2^* = [2(1 + 3d^*/4)T_1^* + (1 + d^*/2)T_i^* + (1 + 3d^*/2)T_o^* + 2(1 + 5d^*/4)T_3^*]/(6 + 6d^*),$$

$$T_3^* = [(1 + d^*)T_1^* + 2(1 + 5d^*/4)T_2^* + (1 + 7d^*/4)T_o^* + 3(1 + 7d^*/4)T_o^*]/(7 + 21d^*/2). \tag{57a}$$

In a manner similar to the rectangular network method, these equations are solved for the dimensionless temperatures.

The heat transfer rate in per unit length Q is given by

$$Q = [K_{p-1}(T_i-T_1) + K_{Q-1}(T_i-T_1) + K_{Q-2}(T_i-T_2)]/e, \quad (58)$$

which, when simplified and nondimensionalized with the values of the thermal conductances from Eqs. (57), reduces to

$$Q^* = (\pi\sqrt{3}) \; [3(1 + d^*/4)(T_i^*-T_1^*) + (1 + d^*/4)(T_i^*-T_1^*) + (1 + d^*/2)(T_o^* - T_2^*)]. \quad (59)$$

Similarly the dimensionless heat transfer rate out per unit length is obtained. The percentage deviations in the dimensionless temperatures and the heat transfer rates compared to the analytical case are calculated as in the last case and are compiled in Table III.

In addition,for the same ratio r_o/r_i this example was solved using one node and two nodes in a manner similar to the method just outlined for three nodes. Figs. 11 and 12 illustrate the networks which were used. The results are also in Table III. The graphs of ε_q versus the size of the element for the rectangular method and for the triangular method with one, two and three nodes are shown in Fig. 13. From Table III and Fig. 13 the following conclusions can be made.

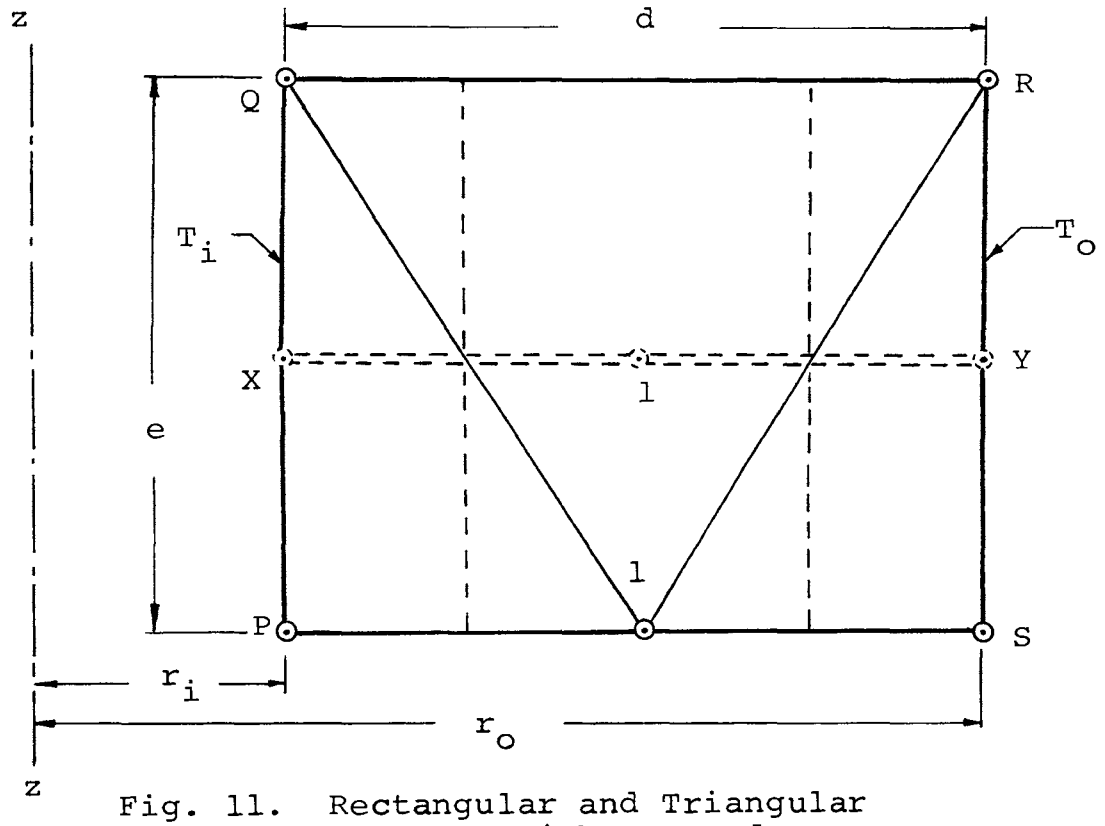

Fig. 11. Rectangular and Triangular Networks with One Node

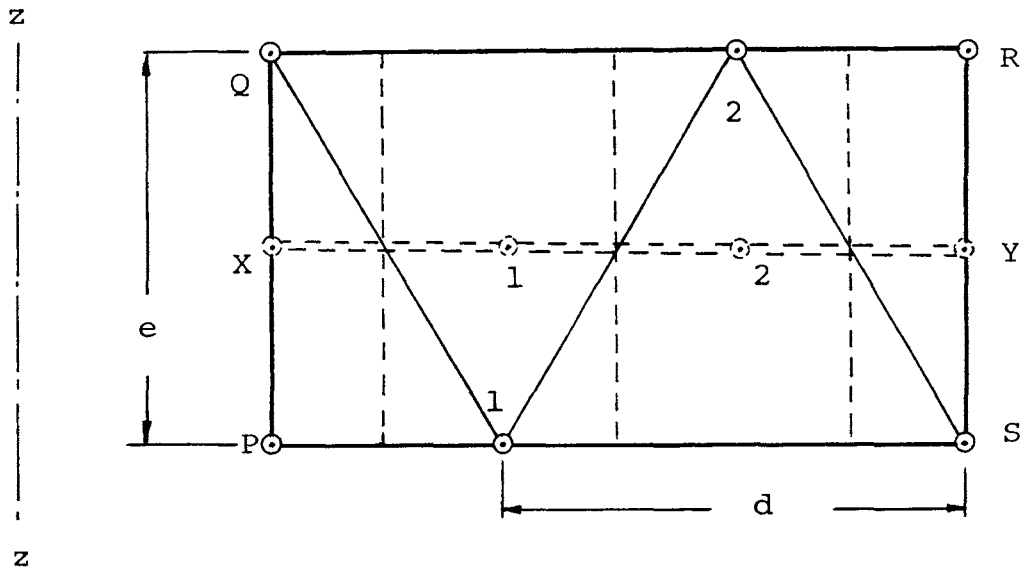

Fig. 12. Rectangular and Triangular Networks with Two Nodes

Table III. Temparatures and Heat Transfer Rates for an Infinitely Long Hollow Cylinder Using Three Methods of Solution

$r_o/r_i=1.36$

d* (N)	Methods	T_1*	T_2*	T_3*	Q*		ε_1	ε_2	ε_3	ε_q	
					in	out				in	out
0.36 (1)	Analytical	.46172			20.43414						
	Rectangular	.46186			20.47507	20.47505	0.014			.200	.200
	Triangular	.46186			20.51501	20.51500	0.014			.396	.396
0.24 (2)	Analytical	.63143	.30043		20.43414						
	Rectangular	.63150	.30047		20.45242	20.45235	0.007	0.005		.089	.089
	Triangular	.63133	.30068		20.47623	20.47620	-0.010	0.026		.206	.206
0.18 (3)	Analytical	.71974	.46172	.22267	20.43414						
	Rectangular	.71976	.46175	.22269	20.44455	20.44431	0.002	0.003	.002	.051	.051
	Triangular	.71968	.46180	.22279	20.45963	20.45950	-0.006	0.008	.012	.125	.125

N: Number of Nodes

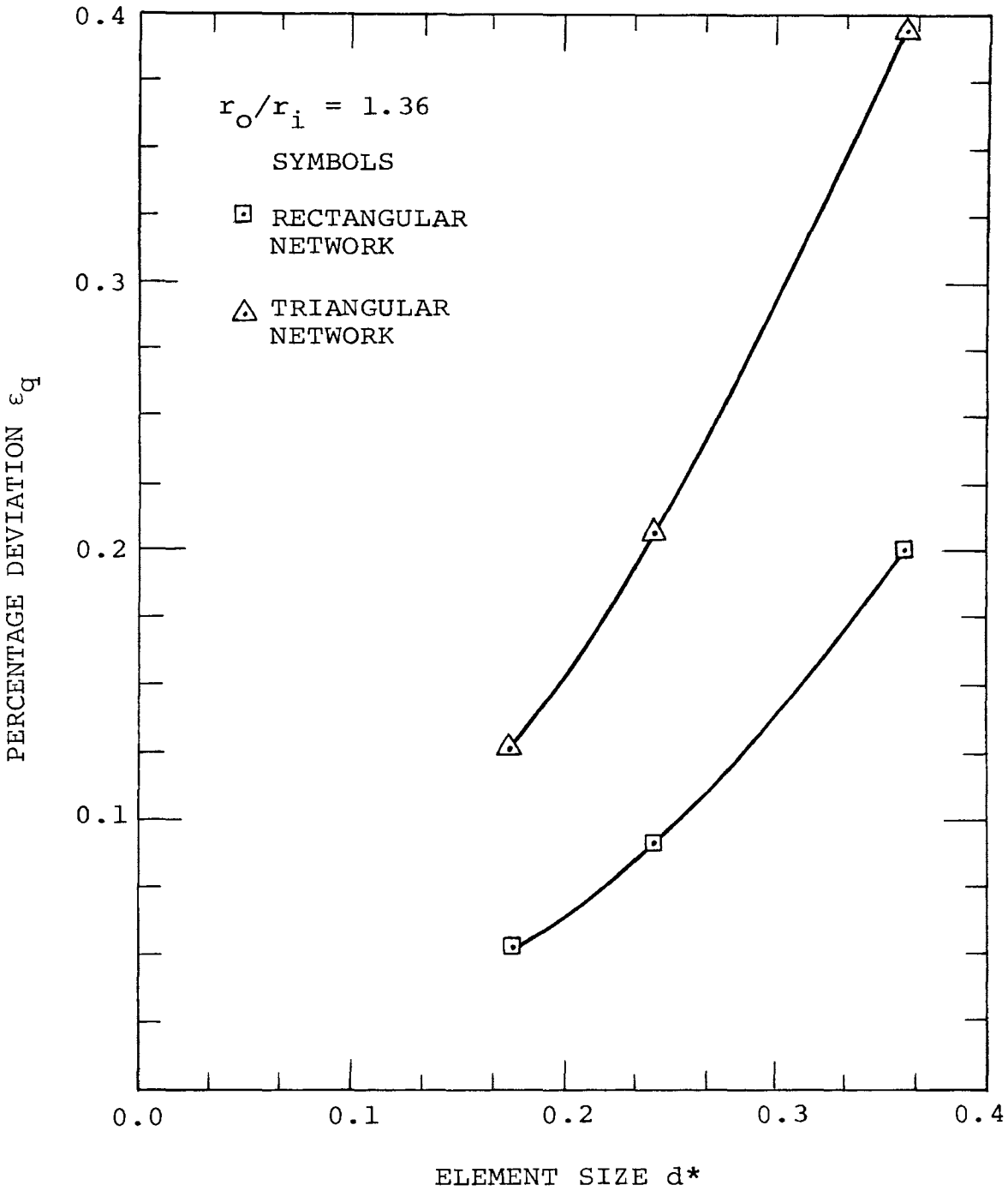

Fig. 13. Deviation in Heat Transfer Rates for Rectangular and Triangular Networks

1. The temperatures obtained by the rectangular and the triangular networks have comparable percentage deviations for every size of element under consideration. For example, corresponding to $d^* = 0.24$ values of ε_1 are 0.007 and -0.010 for the rectangular and triangular networks, respectively. These deviations are well within the requirements of general engineering accuracy.

2. The percentage deviation ε_q for the triangular element has a maximum value of 0.396 compared to 0.200 for the rectangular element, corresponding to $d^* = 0.36$. The value of ε_q for the triangular element is within general engineering accuracy, although it is almost double the value for the rectangular element. The trend of the graphs indicate that the triangular network gives a more rapid decrease in ε_q with a decrease in the element size as compared to the rectangular network. This trend further indicates the validity of the triangular element, because the error diminishes as the network becomes finer.

The second example is subject to convective boundary conditions.

B. A Circular Fin with Rectangular Profile

Fig. 14 illustrates the geometry of the fin under consideration. The results of the triangular network will again be compared with those of a rectangular network and with the analytical method. The fin is assumed to have an insulated end, base temperature and the ambient temperatures of T_i and T_f, respectively, and a constant convective heat transfer coefficient h from the surface of the fin. The problem is analyzed in one dimension.

i. Analytical Method

The differential equation governing the heat conduction in the fin is [7]

$$\frac{d}{dr}\left[k\, A(r)\, \frac{dT}{dr}\right] = \frac{dA_s}{dr}\, h(T - T_f), \qquad (60)$$

where the area for conduction A(r) and the differential area dA_s for convection are

$$A(r) = 2\pi re \text{ and } dA_s = 2(2\pi r\, dr). \qquad (61)$$

Introducing the dimensionless temperature T* and radius r* as

$$T^* = (T - T_f)/(T_i - T_f) \text{ and } r^* = r/r_i, \qquad (62)$$

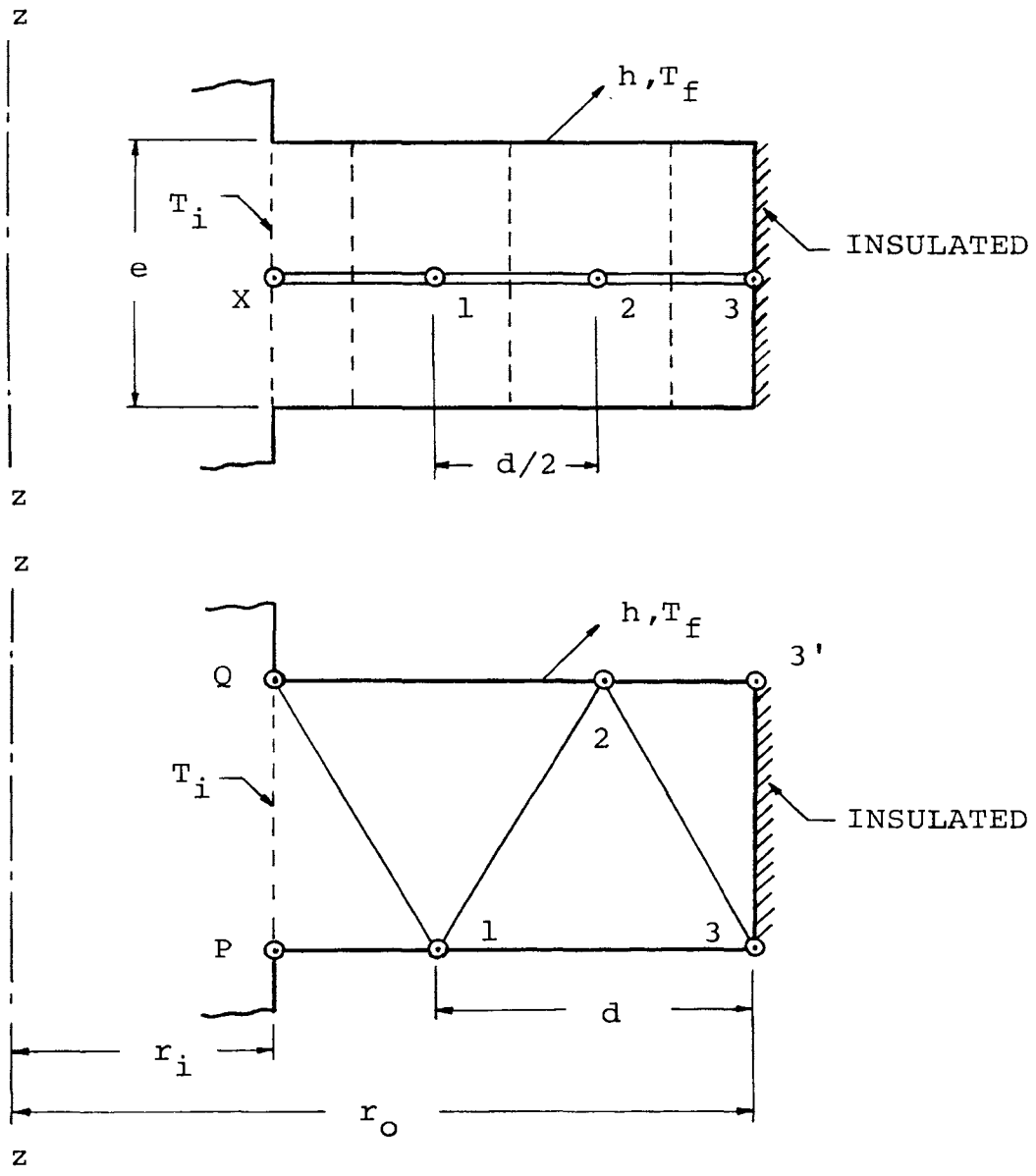

Fig. 14. Rectangular and Triangular Networks in a Circular Fin

Eq. (60) becomes

$$r^{*2} \frac{d^2T^*}{dr^{*2}} + r^* \frac{dT^*}{dr^*} - m^{*2} r^{*2} T^* = 0 \qquad (63)$$

where

$$m^{*2} = [2h/(ke)]r_i^2. \qquad (64)$$

Eq. (63) is a Bessel's equation of order zero. Its solution [5] with the associated boundary conditions

$$T^*(r_i^*) = T_i^*, \quad \frac{dT^*(r_o^*)}{dr^*} = 0, \qquad (65)$$

is

$$T^* = T_i^*[I_0(m^*r^*)K_1(m^*r_o^*)+K_0(m^*r^*)I_1(m^*r_o^*)] / [I_0(m^*r_i^*)K_1(m^*r_o^*)+K_0(m^*r_i^*)I_1(m^*r_o^*)], \qquad (66)$$

where I_0, I_1 and K_0, K_1 are modified Bessel's functions of first and second kind of order zero and one, respectively. The dimensionless temperatures $T_{a_1}^*$, $T_{a_2}^*$ and $T_{a_3}^*$ (subscript a is for analytical case) corresponding to the dimensionless radii r_1^*, r_2^* and r_3^* can now be obtained. The heat transfer rate Q_a^* (i.e. heat lost by the fin) through the base of the fin is

$$Q_a^* = 2\pi e^* m^* T_i^* [K_1(m^*r_i^*)I_1(m^*r_o^*) - I_1(m^*r_i^*) K_1(m^*r_o^*)] / [I_0(m^*r_i^*)K_1(m^*r_o^*)+K_0(m^*r_i^*) I_1(m^*r_o^*)] \qquad (67)$$

where the dimensionless expressions for Q_a^* and e* are

$$Q_a^* = Q_a/[kr_i(T_i-T_f)], \tag{68a}$$

$$e^* = e/r_i. \tag{68b}$$

The temperatures and the heat transfer rates are given in Table IV for three values of m* for a fin of a fixed geometry.

ii. Rectangular Network Method

The network for this method is also shown in Fig. 14. To find the nodal temperatures, an energy balance at each node is performed using the dimensionless temperatures, as defined in Eq. (62). The result is

$$K_{X-1}(T_i^*-T_1^*)+ K_{2-1}(T_2^*-T_1^*)+2h[2\pi(r_i+d/2)(d/2)]$$
$$(T_f^*-T_1^*) = 0,$$

$$K_{1-2}(T_1^*-T_2^*)+K_{3-2}(T_3^*-T_2^*)+2h[2\pi(r_i+d)(d/2)](T_f^*-T_2^*)=0,$$

$$K_{2-3}(T_2^*-T_3^*)+2h[2\pi(r_i+11d/8)(d/4)](T_f^*-T_3^*)=0, \tag{69}$$

The thermal conductance K_{X-1} is

$$K_{X-1} = k[2\pi(r_i+d/4)e/(d/2)], \tag{70}$$

where $d = 2e/\sqrt{3}$. The other thermal conductances are obtained in like manner and are inserted into Eqs.(69) to yield expressions for the dimensionless temperatures. The result is

$$T_1^* = [2(1/d^* + 1/4)T_i^* + 2(1/d^* + 3/4)T_2^* + m^{*2}(1+d^*/2)(d^*/2)T_f^*]/[2(1/d^*+1/4)+2(1/d^*+3/4)+m^{*2}(1+d^*/2)(d^*/2)],$$

$$T_2^* = [2(1/d^*+3/4)T_1^*+2(1/d^*+5/4)T_3^*+m^{*2}(1+d^*)(d^*/2)T_f^*]/[2(1/d^*+3/4)+2(1/d^*+5/4)+m^{*2}(1+d^*)(d^*/2)],$$

$$T_3^* = [2(1/d^*+5/4)T_2^*+m^{*2}(1+11d^*/8)(d^*/4)T_f^*]/[2(1/d^*+5/4)+m^{*2}(1+11d^*/8)(d^*/4)], \quad (71)$$

where $d^* = d/r_i$.

The above equations are solved for the dimensionless temperatures. The heat transfer rate in at the base is written as

$$Q = K_{X-1}(T_i-T_1)+2h[2\pi(r_i+d/8)(d/4)](T_i-T_f), \quad (72)$$

which, when simplified and nondimensionalized with the aid of Eq. (70), reduces to

$$Q^* = 2\pi e^*[2(1/d^*+1/4)(T_i^*-T_1^*)+m^{*2}(1+d^*/8)(d^*/4)(T_i^*-T_f^*)], \quad (73)$$

where Q* is defined in Eq. (68a). The dimensionless heat loss by convection Q* is similarly found to have the expression

$$Q^* = 2\pi e^* m^{*2}[(1+d^*/8)(d^*/4)(T_i^*-T_f^*)+(1+d^*/2)(d^*/2)(T_1^*-T_f^*)+(1+d^*)(d^*/2)(T_2^*-T_f^*)+(1+11d^*/8)(d^*/4)(T_3^*-T_f^*)]. \quad (74)$$

Eqs. (73) and (74) will give the same value of Q*. The percentage deviations ε_1, ε_2 and ε_3 in the dimensionless temperatures are obtained from Eq. (54). The percentage deviations ε_q in the dimensionless heat transfer rates are obtained by using Eqs. (55),(73),(74), and are compiled in Table IV.

iii. Triangular Network Method

Fig. 13 illustrates the triangular network used. The nodes are positioned at the same radius as in the rectangular network method for direct comparison of temperatures. Regular triangular elements are selected so that the conductances can be computed with ease. The representative element size d is taken as

$$d = 2e/\sqrt{3} \ . \quad (75)$$

Performing an energy balance at each node in terms of the dimensionless temperatures gives

$$K_{P-1}(T_i^*-T_1^*)+K_{Q-1}(T_i^*-T_1^*)+K_{2-1}(T_2^*-T_1^*)+K_{3-1}(T_3^*-T_1^*)$$
$$+h[2\pi(r_i+d/2)(3d/4)](T_f^*-T_1^*) = 0,$$

$$K_{1-2}(T_1^*-T_2^*)+K_{Q-2}(T_i^*-T_2^*)+K_{3-2}(T_3^*-T_2^*)+K_{3-2}(T_3^*-T_2^*)$$
$$+h[2\pi(r_i+d)(3d/4)](T_f^*-T_2^*) = 0,$$

$$K_{1-3}(T_1^*-T_3^*)+K_{2-3}(T_2^*-T_3^*)+K_{2-3'}(T_2^*-T_3^*)+h[2\pi(r_i+$$
$$5d/4)(d/2)+2\pi(r_i+11d/8)(d/4)](T_f^*-T_3^*) = 0. \qquad (76)$$

The thermal conductances are

$$K_{P-1}=k[2\pi(r_i+d/4)(e/2)/(d/2)],$$
$$K_{Q-1}=k[2\pi(r_i+d/4)(e/3)/d],$$
$$K_{2-1}=k[2\pi(r_i+3d/4)(2e/3)/d]. \qquad (77)$$

Introducing the expressions for all the conductances into Eqs. (76) and solving the resulting equations yields the expressions

$$T_1^* = [2(1/d^*+1/4)T_i^*+(2/3)(1/d^*+1/4)T_i^*+(4/3)(1/d^*$$
$$+3/4)T_2^*+(2/3)(1/d^*+1)T_3^*+m^{*2}(1+d^*/2)(3d^*/4)T_f^*]$$
$$/[2(1/d^*+1/4)+(2/3)(1/d^*+1/4)+(4/3)(1/d^*+3/4)$$
$$+m^{*2}(1+d^*/2)(3d^*/4)],$$

$$T_2^* = [(4/3)(1/d^*+3/4)T_1^* + (2/3)(1/d^*+1/2)T_i^* + 2(1/d^* + 5/4)T_3^* + (2/3)(1/d^*+5/4)T_3^* + m^{*2}(1+d^*)(3d^*/4) T_f^*]/[(4/3)(1/d^*+3/4) + (2/3)(1/d^*+1/2) + 2(1/d^*+5/4) + (2/3)(1/d^*+5/4) + m^{*2}(1+d^*)(3d^*/4)],$$

$$T_3^* = [(2/3)(1/d^*+1)T_1^* + (2/3)(1/d^*+5/4)T_2^* + 2(1/d^* + 5/4)T_2^* + m^{*2}((1+5d^*/4)(d^*/2) + (1+11d^*/8)(d^*/4)) T_f^*]/[(2/3)(1/d^*+1) + (2/3)(1/d^*+5/4) + 2(1/d^* + 5/4) + m^{*2}((1+5d^*/4)(d^*/2) + (1+11d^*/8)(d^*/4))]. \quad (78)$$

Assigning values to d* and m*, the above equations were solved for the dimensionless nodal temperatures. The heat transfer rate in at the base is given by

$$Q = K_{P-1}(T_i - T_1) + K_{Q-1}(T_i - T_1) + K_{Q-2}(T_i - T_2) + h[2\pi(r_i + d/8)(d/4) + 2\pi(r_i + d/4)(d/2)](T_i - T_f). \quad (79)$$

The expressions for thermal conductances are used from Eqs.(77) and the definition of Q* is introduced, giving

$$Q^* = \pi e^*[2(1/d^*+1/4)(T_i^* - T_1^*) + (2/3)(1/d^*+1/4)(T_i^* - T_1^*) + (2/3)(1/d^*+1/2)(T_i^* - T_2^*) + m^{*2}((1+d^*/8)(d^*/4) + (1+d^*/4)(d^*/2))(T_i^* - T_f^*)]. \quad (80)$$

In a similar manner, the dimensionless heat loss by convection Q* is found to have the expression

$$Q^* = \pi e^* m^{*2}[(1+d^*/8)(d^*/4)(T_i^*-T_f^*)+(1+d^*/4)(d^*/2)(T_i^*-T_f^*)+(1+d^*/2)(3d^*/4)(T_1^*-T_f^*)+(1+d^*)(3d^*/4)(T_2^*-T_f^*)+(1+5d^*/4)(d^*/2)(T_3^*-T_f^*)+(1+11d^*/8)(d^*/4)(T_3^*-T_f)]. \quad (81)$$

The percentage deviations ε_1, ε_2, ε_3 in the dimensionless temperatures are evaluated using relations similar to Eq. (54). The percentage deviations ε_q in the dimensionless heat transfer rates are obtained by Eq. (55). These results are listed in Table IV.

The following conclusions can be drawn from the results:

1. The graph in Fig. 15 shows that the temperatures, obtained by the rectangular and triangular network methods, are very close. For example when d*=0.4 and m*=1.5, the dimensionless temperatures T_2^* having maximum deviation are 0.69635 and 0.70533 for the rectangular and triangular networks,respectively.

2. It is observed in Fig. 16 that the percentage deviation in the heat transfer rate for the triangular network method is 0.333% for m*=0.5.

Table IV. Temperatures and Heat Transfer Rates for a Circular Fin by Three Methods of Solution

$d^*=0.4$

m^*	Methods	T_1^*	T_2^*	T_3^*	Q^*		ε_1	ε_2	ε_3	ε_q	
					in	loss				in	loss
0.5	Analytical	.97071	.95446	.94968	.40905						
	Rectangular	.97057	.95463	.94972	.40946	.40943	-.014	.017	.004	.099	0.093
	Triangular	.97172	.95575	.95001	.41041	.41041	.101	.129	.033	.333	.333
1.0	Analytical	.89428	.83816	.82092	1.47795						
	Rectangular	.89504	.83928	.82228	1.48500	1.48498	.076	.112	.136	.478	.477
	Triangular	.89909	.84361	.82371	1.49941	1.49940	.481	.545	.279	1.453	1.453
1.5	Analytical	.79759	.69360	.66218	2.88132						
	Rectangular	.79954	.69635	.66541	2.91391	2.91389	.195	.275	.323	1.131	1.130
	Triangular	.80694	.70533	.66902	2.97788	2.97788	.935	1.173	.684	3.351	3.351

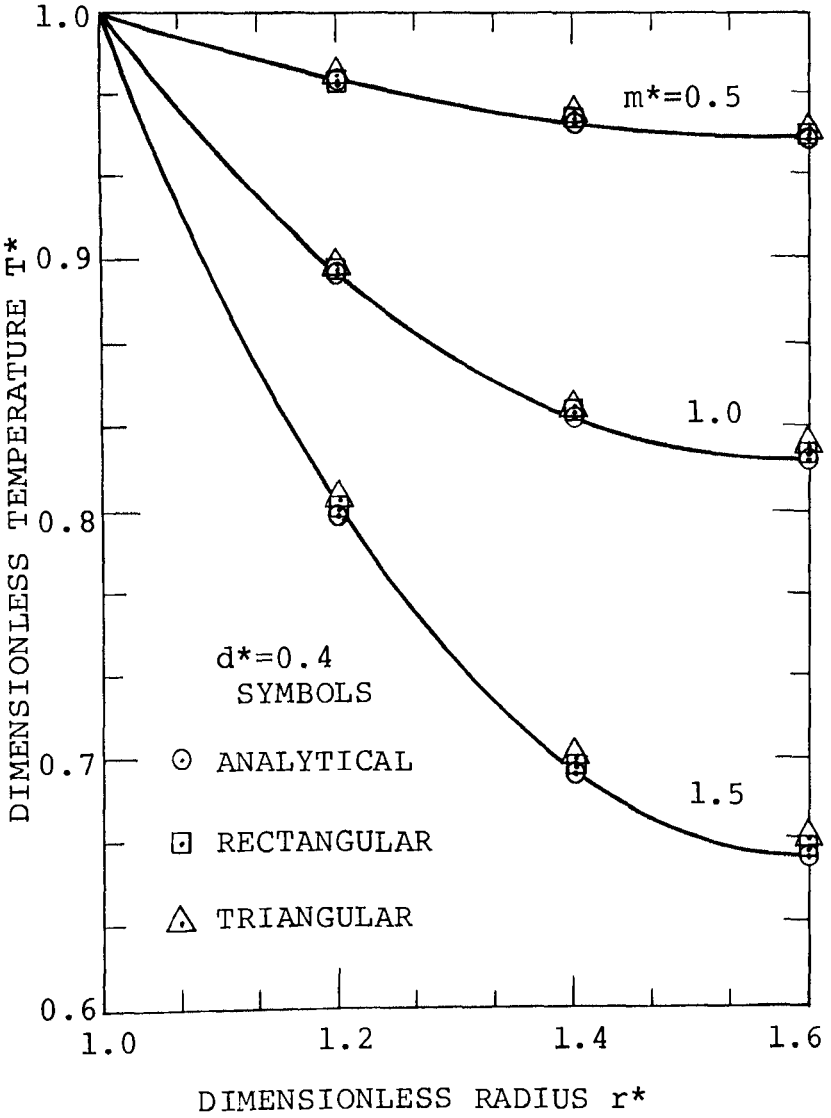

Fig. 15. Temperature Distribution in a Circular Fin by Three Methods

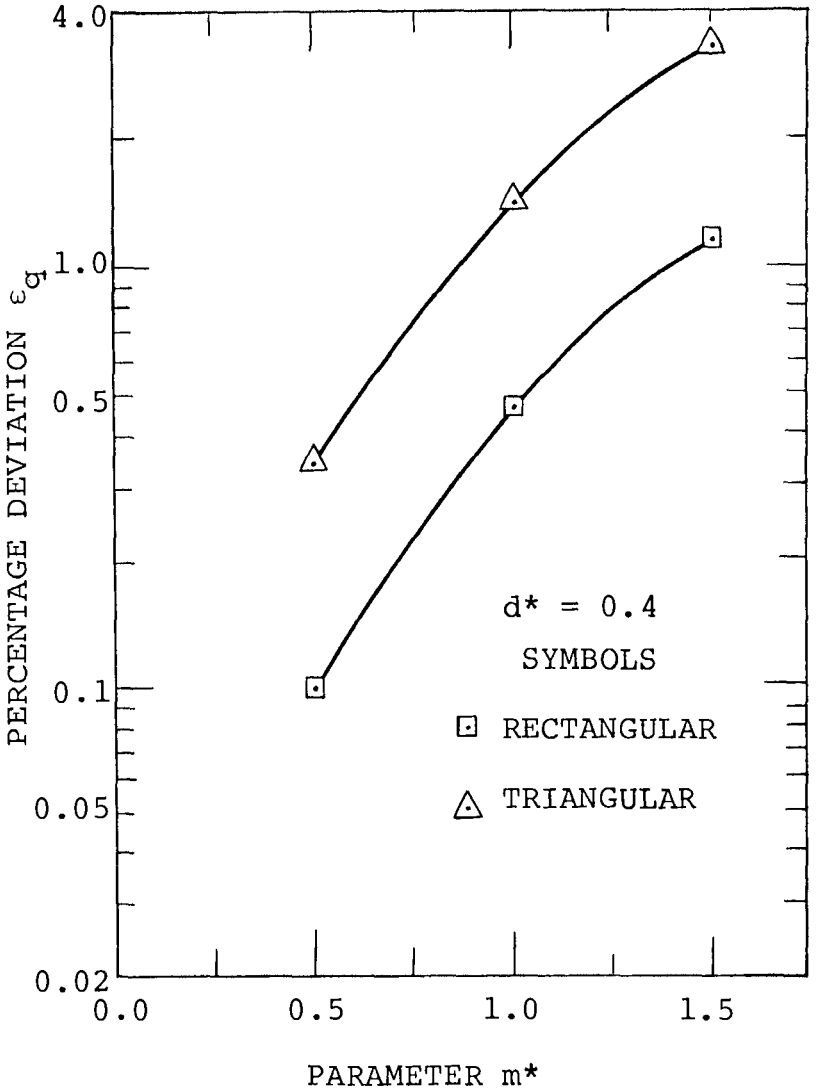

Fig. 16. Comparison of Deviation in Heat Transfer Rates for Rectangular and Triangular Network Methods

However, for higher values of m* the temperature gradient at the base of the fin is large and this introduces more error in both the rectangular and the triangular network methods. The percentage deviation in the triangular network method can be maintained within required workable limits although it is found to be almost three times that of the rectangular network method.

Thus far only one dimensional examples have been discussed. A two dimensional problem will now be analyzed.

C. A Solid Cylinder of Finite Length

In the last two examples, the triangular network forces the heat transfer to take place in an unnatural direction. This may be responsible for the superior accuracy of the rectangular network method in examples A and B. Thus to investigate the suitability of the triangular network in a two dimensional example is the purpose of this discussion.

The assumptions, stated earlier, are employed for this example. The following dimensions are selected for convenience.

$$d = r_o/3, \quad e = \sqrt{3}\, d/2, \quad L = 4e. \tag{82}$$

The cylindrical surface and one of the faces are maintained at a constant temperature T_o. The second face has the impressed axisymmetric temperature distribution f(r) as shown in Fig. 17. A suitable expression for f(r) will be chosen later.

i. Analytical Method

The differential equation governing the heat conduction in the solid finite cylinder is [7]

$$\frac{\partial^2 T}{\partial r^2} + \frac{1}{r}\frac{\partial T}{\partial r} + \frac{\partial^2 T}{\partial z^2} = 0. \tag{83}$$

The boundary conditions are

$$T(r,0) = T_o,\ T(r,L) = f(r),\ T(r_o,z) = T_o,$$
$$T(r,z) \text{ is finite.} \tag{84}$$

The temperature T_o is constant. The dimensionless quantities

$$T^* = (T-T_o)/(T_{ref}-T_o),\ r^* = r/r_o,\ z^* = z/L \text{ and}$$
$$P^* = r_o/L, \tag{85}$$

are introduced where T_{ref} is the value of f(0). Separation of variables was used to solve this boundary value problem. The result is

$$T^*(r^*,z^*) = J_0(\lambda_1 * r^*)\sinh(P^*\lambda_1 * z^*)/\sinh(P^*\lambda_1 * L^*), \tag{86}$$

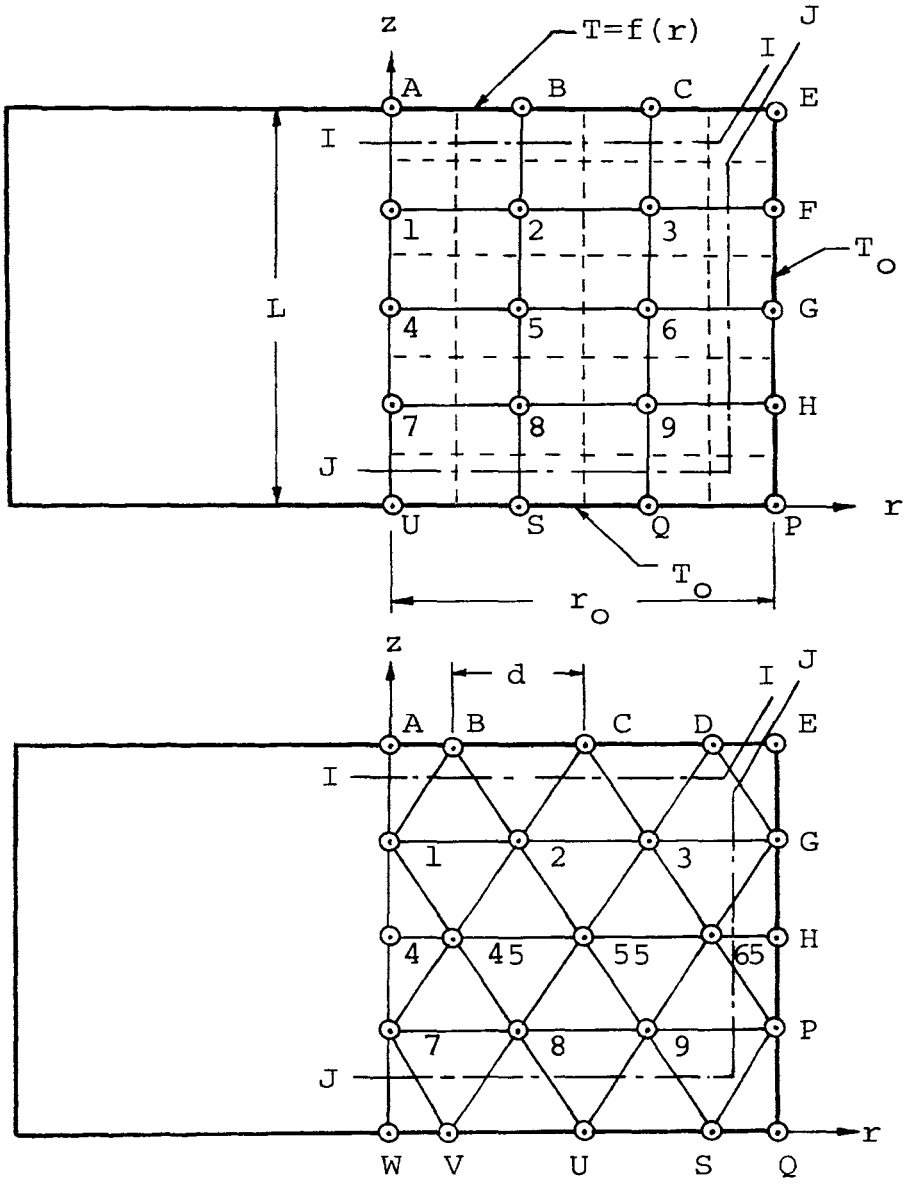

Fig. 17. Rectangular and Triangular Networks in a Finite Solid Circular Cylinder

if f(r) is taken as

$$f(r) = (T_{ref}-T_o)\ J_0(\lambda_1 * r^*) + T_o. \qquad (87)$$

The symbol $\lambda_1 *$ is the first eigenvalue of the characteristic equation

$$J_0(\lambda_n * L^*) = 0, \qquad (88)$$

and J_0 is the Bessel's function of the first kind of order zero. The dimensionless temperatures are evaluated by Eq. (86) with suitable values of r* and z* and are denoted by $T_a *$. The heat transfer rate in Q_a through the top face of the cylinder (z=L) is given by

$$Q_a = k \int_0^{r_o} \frac{\partial T}{\partial z} \cdot 2\pi r dr, \qquad (89)$$

which has the dimensionless form

$$Q_a * = (2\pi\ r_o{}^2/L) \int_0^1 \frac{\partial T^*}{\partial z^*}\ r^*\ dr^*, \qquad (90)$$

where $Q_a *$ is

$$Q_a * = Q_a/[ke(T_{ref}-T_o)]. \qquad (91)$$

Substituting $\frac{\partial T^*}{\partial z^*}$, obtained from Eq. (86), into Eq. (90) and integrating, yields

$$Q_a * = 8\pi J_1(\lambda_1 *)\cosh(P^*\lambda_1 *)/\sinh(P^*\lambda_1 *). \qquad (92)$$

The values of λ_1^* and $J_1(\lambda_1^*)$ are available in standard tables of Bessel's functions.

ii. Rectangular Network Method

The network for this method is shown in Fig. 17. An energy balance is again performed at each node and the conductances are expressed in terms of d and e. When the values of the conductances are introduced into the set of energy balance equations, the result in terms of the dimensionless temperatures is

$$T_1^* = (T_A^* + 3T_2^* + T_4^*)/5, \quad T_2^* = (8T_B^* + 9T_3^* + 8T_5^* + 3T_1^*)/28,$$

$$T_3^* = (16T_C^* + 15T_o^* + 16T_6^* + 9T_2^*)/56, \quad T_4^* = (T_1^* + 3T_5^* + T_7^*)/5,$$

$$T_5^* = (8T_2^* + 9T_6^* + 8T_8^* + 3T_4^*)/28, \quad T_6^* = (16T_3^* + 15T_o^* + 16T_9^* + 9T_5^*)/56,$$

$$T_7^* = (T_4^* + 3T_8^* + T_o^*)/5, \quad T_8^* = (8T_5^* + 9T_9^* + 8T_o^* + 3T_7^*)/28,$$

$$T_9^* = (16T_6^* + 15T_o^* + 16T_o^* + 9T_8^*)/56. \tag{93}$$

These equations are solved for the dimensionless temperature where T_A^*, T_B^*, T_C^* and T_o^* are defined by Eqs.(87) and (85). The dimensionless heat transfer rate Q* across the section I-I (Fig. 17) is found in a manner similar to the last two examples. The expression is

$$Q^* = (\pi/6)[2(T_A^*-T_1^*)+16(T_B^*-T_2^*)+32(T_C^*-T_3^*)+15(T_C^*-T_o^*)] \quad (94a)$$

Similarly, the dimensionless heat transfer rate across the section J-J is found to be

$$Q^* = \pi[(5/2)T_C^*+5(T_3^*+T_6^*+T_9^*)+(1/3)(16T_9^*+8T_8^*+T_7^*)]. \quad (94b)$$

The dimensionless heat transfer rate is defined in a manner similar to Eq. (91). The percentage deviations ε in the dimensionless temperatures are obtained by using expressions similar to Eq. (54). The percentage deviations ε_q in the dimensionless heat transfer rates are evaluated by using Eq. (55). The results of the computation are given in Table V.

iii. Triangular Network Method

The network, as shown in Fig. 17, is constructed such that the total number of nodes is 10, compared to 9 in the rectangular network. All the nodes except the nodes 45, 55 and 65 are positioned in identical locations for direct comparison of the temperatures with the rectangular network method. The thermal conductances are again easily expressed in terms of d and e. The simplification of the non-dimensional form of the set of energy balance equations results in

$$T_1^* = (T_A^*+2T_B^*+8T_2^*+2T_{45}^*+T_4)/14,$$

$$T_2^* = (2T_1^*+3T_B^*+5T_C^*+6T_3^*+5T_{55}^*+3T_{45}^*)/24,$$

$$T_3^* = (6T_2^*+7T_C^*+9T_D^*+10T_o^*+9T_{65}^*+7T_{55}^*)/48,$$

$$T_4^* = (T_1^*+12T_{45}^*+T_7^*)/14,$$

$$T_{45}^* = (6T_4^*+T_1^*+6T_2^*+8T_{55}^*+6T_8^*+T_7^*)/28,$$

$$T_{55}^* = (4T_{45}^*+5T_2^*+7T_3^*+8T_{65}^*+7T_9^*+5T_8^*)/36,$$

$$T_{65}^* = (16T_{55}^*+18T_3^*+11T_o^*+66T_o^*+11T_o^*+18T_9^*)/140,$$

$$T_7^* = (T_4^*+2T_{45}^*+8T_8^*+2T_o^*+T_o^*)/14,$$

$$T_8^* = (2T_7^*+3T_{45}^*+5T_{55}^*+6T_9^*+5T_o^*+3T_o^*)/24,$$

$$T_9^* = (6T_8^*+7T_{55}^*+9T_{65}^*+10T_o^*+9T_o^*+7T_o^*)/48, \tag{95}$$

where T_A^*, T_B^*, T_C^*, T_D^* and T_o^* are defined by Eqs. (87) and (85) The above equations were solved for the nodal temperatures. The dimensionless heat transfer rate Q* across the section I-I (Fig. 17) is given by

$$Q^* = (\pi/12)[(T_A^*-T_1^*)+2(T_B^*-T_1^*)+12(T_B^*-T_2^*)+20(T_C^*-T_2^*)+28(T_C^*-T_3^*)+36(T_D^*-T_3^*)+88(T_D^*-T_o^*). \tag{96a}$$

Similarly, the expression for the dimensionless heat transfer rate Q* across the section J-J is found to be

$$Q^* = (\pi/12)[88T_D^* + 40T_3^* + 176T_{65}^* + 104T_9^* + 32T_8^* + 3T_7^*]. \quad (96b)$$

The percentage deviations in the dimensionless temperatures and in the heat transfer rates in Eqs. (96a) and (96b) are evaluated in a manner similar to the rectangular network method. The results are given in Table V. Figs.18 and 19 illustrate the temperature distribution and the percentage deviations in the temperatures which result from the calculations.

The following conclusions can be drawn from this example.

1. The percentage deviations in the dimensionless temperatures obtained by the triangular network method are smaller than those obtained by the rectangular network method. The maximum percentage deviation ε is -0.344% for the triangular network as compared to 1.422% for the rectangular network method.

2. Table V gives the percentage deviation in the heat transfer rate as 3.210% for the triangular network method, whereas for the rectangular method the figure is -0.899%. They are comparable values.

Table V. Temperatures and Heat Transfer Rates for a Solid Cylinder by Three Methods of Solution

$d/r_o = 1/3$

Node No.	Position		Analytical	Rectangular		Triangular	
	r*	z*	T_a*	T*	ε	T*	ε
1	0	3/4	0.49360	0.50782	1.422	0.49541	0.181
2	2/6	3/4	0.41742	0.43037	1.295	0.41737	-0.005
3	4/6	3/4	0.22385	0.23101	0.716	0.22411	0.026
4	0	2/4	0.23483	0.24797	1.314	0.23238	-0.245
45	1/6	2/4	0.22548			0.22204	-0.344
5	2/6	2/4	0.19859	0.21033	1.174		
55	3/6	2/4	0.15731			0.15706	-0.025
6	4/6	2/4	0.10650	0.11297	0.647		
65	5/6	2/4	0.05204			0.05224	0.020
7	0	1/4	0.09387	0.10103	0.716	0.09340	-0.047
8	2/6	1/4	0.07938	0.08572	0.634	0.07890	-0.048
9	4/6	1/4	0.04257	0.04605	0.348	0.04256	-0.001
Sections			Q_a*	Q*	ε_q	Q*	ε_q
I-I			11.38635	11.28405	-0.898	11.75191	3.211
J-J				11.28394	-0.899	11.75189	3.210

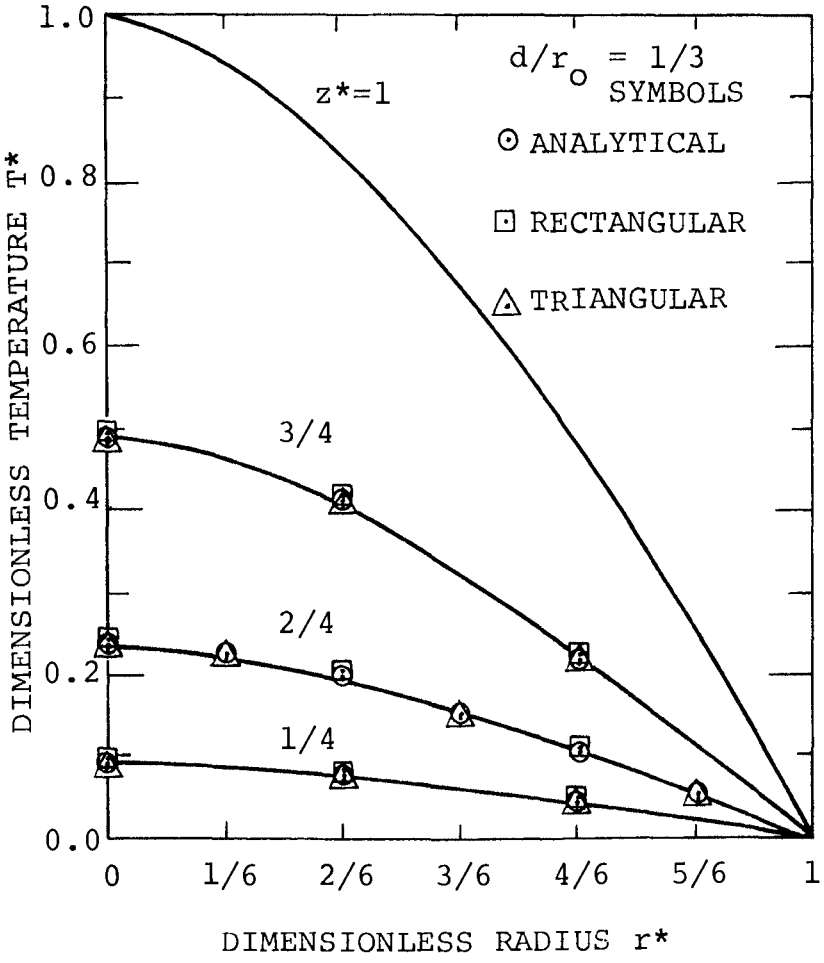

Fig. 18. Temperature Distribution in a Solid Cylinder of Finite Length by Three Methods

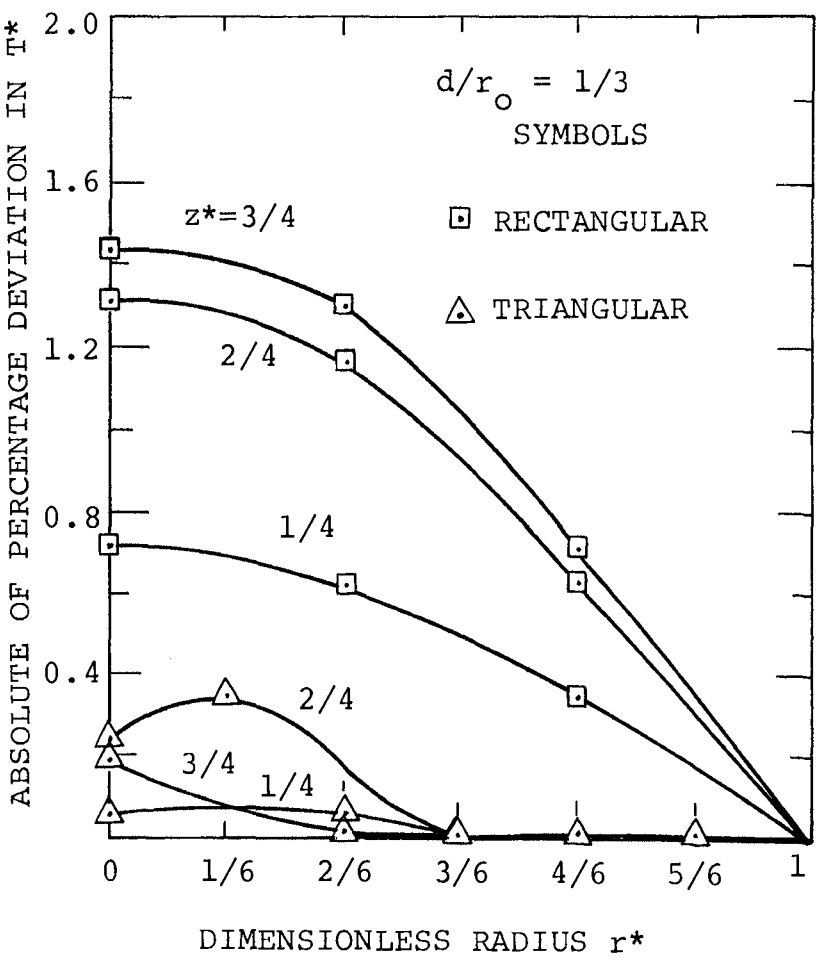

Fig. 19. Deviations in the Dimensionless Temperatures by Two Methods for a Solid Cylinder of Finite Length

V. AN INDUSTRIAL APPLICATION

The previous chapters show that the triangular network with the proposed triangular element gives results which are comparable to that of the rectangular network. Many other favorable aspects of the triangular network are of vital importance in practical problems. Some of these are

1. The triangular network fits an irregular axisymmetric geometry with ease.

2. It can be used to connect a fine network with a fine or a coarse network, regardless of the types of element employed. For example, a fine network of rectangular elements can be connected with a fine or a coarse network consisting of polar elements by using the triangular element.

The application which follows highlights the useful features of the proposed triangular element. This problem was previously solved employing the finite element method[8].

A tall cylindrical reaction vessel with a hemispherical bottom, erected by a weld joint on a cylindrical skirt, is shown in Fig. 20. The skirt and the vessel are insulated and the temperature on the inner side of the vessel is 650 ^{o}F. The ambient temperature outside the vessel is 0^{o}F. The conductivity of the vessel, the skirt

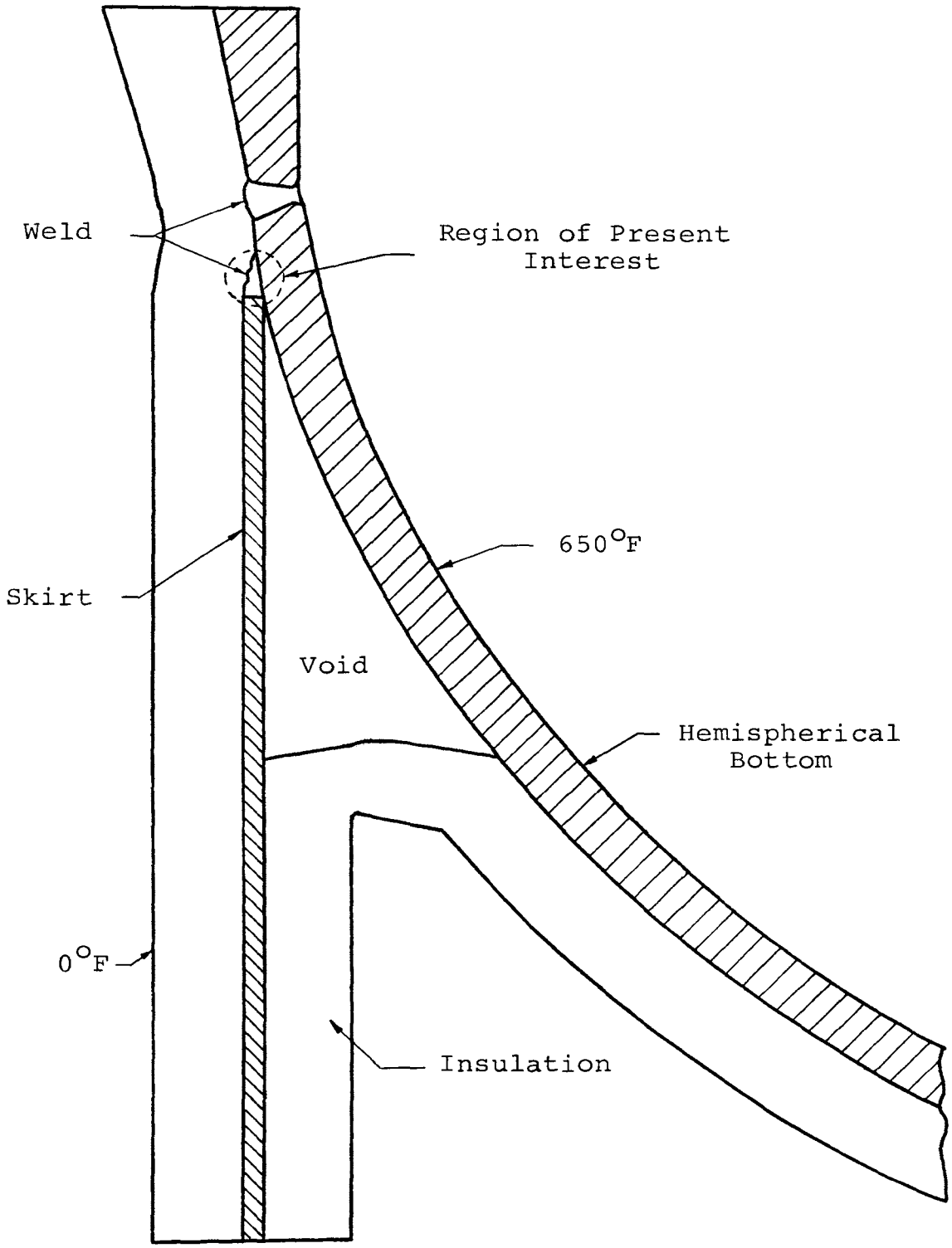

Fig. 20. Section of the Bottom of a Reaction Vessel

and the weld is .043 Btu/min.in.^{o}F. The bottom of the reaction vessel, specially in the vicinity of the weld joint, must be tested for thermal stress. The temperature distribution is required for this reason. The previous solution used the finite element method to find the temperatures at 703 nodal points, which were distributed over the bottom of the reaction vessel in such a way that the regions of stress concentration had nodal points closer to each other. The number of elements was 617, and included rectangular, triangular, polar and other general shapes. The details of the finite element method are not of interest here.

For the present purpose of illustrating the application of the proposed triangular element, a portion of the hemispherical bottom is chosen for convenience. The weld joint is suitable for highlighting the two main advantages of the triangular network. The enlarged view of the weld joint in Fig. 21 shows the positioning of triangular elements along the irregular boundary on the outerside. One row of polar elements on the innerside are matched with the rectangular elements by the use of triangular elements. For comparison with the finite element method, all the nodal points except node 176 are positioned in identical locations. Nodal points 165 and 174 are omitted by the introduction of the new node 176 at a central position.

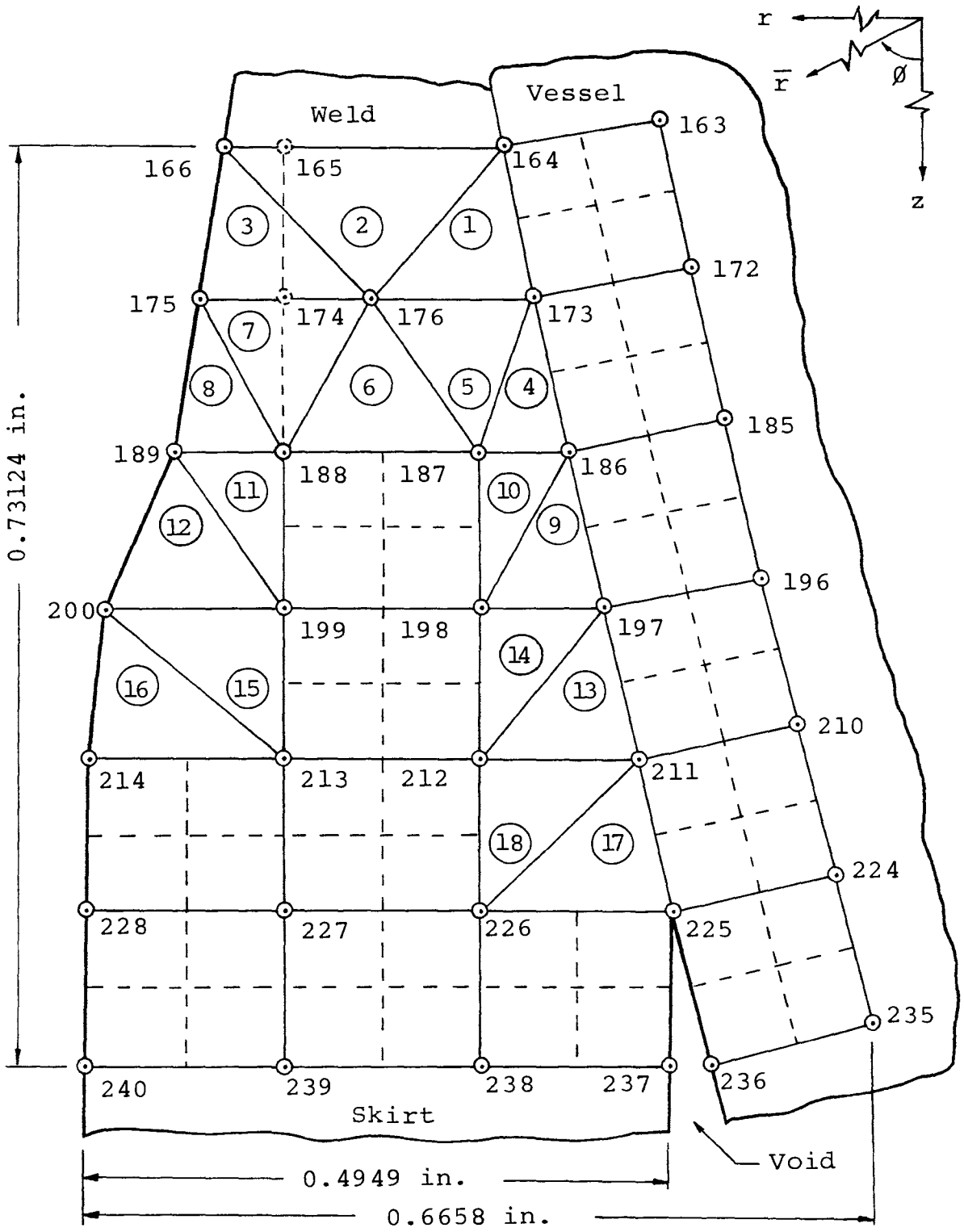

Fig. 21. Use of the Triangular Network in an Irregular Weld Joint

With the network so constructed, the example was solved to find the nodal temperatures. The results of the finite element method are used as boundary conditions in the present analysis. An energy balance was performed at each of the 14 nodes in the region of interest. Although the process is tedious, the principle is the same as the last three examples. The thermal conductances are the basic quantities involved in the energy balance equations. Of the 45 different thermal conductances that are required, only 8 distinct expressions exist. These 8 representative expressions are

1. $K_{173-176}=\pi k[(r_{173}+r_{176})/d_{173-176}](p^1_{173-176} + p^5_{173-176})$,

2. $K_{164-173}=\pi k[(r_{164}+r_{173})/d_{164-173}](p^1_{164-173} + \Delta\bar{r}/2)$,

3. $K_{172-173}=\pi k[(r_{172}+r_{173})/d_{172-173}](\bar{r}_m\Delta\emptyset)$,

4. $K_{187-188}=\pi k[(r_{187}+r_{188})/d_{187-188}](p^6_{187-188} + d_{187-198}/2)$,

5. $K_{198-199}=\pi k[(r_{198}+r_{199})/d_{198-199}][(d_{187-198} + d_{212-198})/2]$,

$$6.\quad K_{225-236}=\pi k[(r_{225}+r_{236})/d_{225-236}](\Delta\bar{r}/2),$$

$$7.\quad K_{225-237}=\pi k[(r_{225}+r_{237})/d_{225-237}](d_{225-226}/2),$$

$$8.\quad K_{166-175}=\pi k[(r_{166}+r_{175})/d_{166-175}](p^{3}_{166-175}).$$

(97)

In these equations, d_{m-n} is the distance between the nodes m and n, p^{i}_{m-n} is the length of the perpendicular bisector of the side m-n of the triangular element i, $\Delta\bar{r}$ is the size of the polar elements in terms of the difference of the spherical radii of the two faces of the element, $\bar{r}_m$ is the mean spherical radius of the polar elements and $\Delta\emptyset$ is the angular increment of each of the polar elements. The energy balance equations were solved for the 14 nodal temperatures. Denoting the temperatures obtained by finite element method by T_{fe}, the percentage difference in T and T_{fe} is expressed as

$$\delta = [(T-T_{fe})/(T_{max}-T_{min})]100, \tag{98}$$

where the maximum and the minimum temperatures T_{max} and T_{min}, respectively, in the region of present interest are

$$T_{max} = 645.905, \quad T_{min} = 638.247. \tag{99}$$

Table VI lists the results of the finite element method and the temperatures from the present analysis. The last column gives δ.

Table VI. Comparison of the Finite Difference and Finite Element Methods

Node Nos.	r inch	z inch	$\bar{r}$ inch	ϕ radian	Finite Element T_{fe} Degree F	Finite Difference T Degree F	Percent Difference δ
163	29.2399	6.28002	29.90668	1.35923	645.905		
164	29.3927	6.31283	30.06297	1.35923	645.324		
166	29.6497	6.31283	- -	- -	644.855		
172	29.2136	6.40155	29.90674	1.35508	645.549		
173	29.3662	6.43499	30.06296	1.35508	644.824	644.826	0.022
176	29.5196	6.43499	- -	- -	- -	644.366	- -
175	29.6730	6.43499	- -	- -	644.021		
185	29.1867	6.52296	29.90672	1.35092	645.218		
186	29.3392	6.55704	30.06299	1.35092	644.312	644.320	0.105
187	29.4187	6.55704	- -	- -	643.967	643.965	-0.022
188	29.5864	6.55704	- -	- -	643.360	643.361	0.006
189	29.6954	6.55704	- -	- -	643.074		

Table VI (Continued)

Node Nos.	r inch	z inch	$\bar{r}$ inch	ϕ radian	T_{fe} degree F	T degree F	δ
196	29.1593	6.64426	29.90669	1.34676	644.947		
197	29.3117	6.67897	30.06300	1.34676	643.795	643.813	0.230
198	29.4187	6.67897	- -	- -	643.159	643.161	0.032
199	29.5864	6.67897	- -	- -	642.419	642.423	0.048
200	29.7450	6.67897	- -	- -	641.952		
210	29.1314	6.76544	29.90666	1.34260	644.821		
211	29.2836	6.80079	30.06293	1.34260	643.290	643.324	0.443
212	29.4187	6.80079	- -	- -	642.159	642.179	0.261
213	29.5864	6.80079	- -	- -	641.313	641.351	0.491
214	29.7500	6.80079	- -	- -	640.985		
224	29.1031	6.88651	29.90675	1.33844	645.074		
225	29.2551	6.92249	30.06294	1.33844	642.851	642.904	0.689

Table VI (Continued)

Node Nos.	r inch	z inch	$\bar{r}$ inch	ϕ radian	T_{fe} Degree F	T Degree F	δ
226	29.4187	6.92249	- -	- -	640.734	640.886	1.983
227	29.5864	6.92249	- -	- -	639.995	640.040	0.580
228	29.7500	6.92249	- -	- -	639.735		
235	29.0742	7.00746	29.90674	1.33429	645.642		
236	29.2261	7.04407	30.06299	1.33429	645.115		
237	29.2551	7.04407	- -	- -	639.487		
238	29.4187	7.04407	- -	- -	638.991		
239	29.5864	7.04407	- -	- -	638.447		
240	29.7500	7.04407	- -	- -	638.247		

It is observed that the results, obtained by using the proposed triangular element together with the rectangular and polar networks, are very close to those obtained by the finite element method. The percentage difference ranges from 0.006% to 1.983%.

VI. CONCLUSION

A study of the three feasible definitions for the geometric factors of the proposed triangular element indicates that the formulation based on the mid-radius of each side of the triangle (case 3) is the preferred definition. This formulation yields a resultant thermal conductance which best agrees with the thermal conductances for a rectangular element.

The geometric factor for the triangular elements in two dimensional cylindrical coordinates approaches that for the rectangular element as the size of the elements are decreased. This establishes the validity of the triangular elements and hence the triangular network.

The triangular elements yield a resultant geometric factor which closely agrees with the geometric factor for the rectangular element based on the logarithmic mean area. The percentage deviation between the resultant geometric factor for the triangular elements and the geometric factor for rectangular element based on the logarithmic mean area is less than the percentage deviation between the geometric factor for the rectangular element based on the arithmetic mean area and the geometric factor based on the logarithmic mean area. This conclusion is true regardless of the shape of the

triangular elements. This indicates the workability of the triangular network using the proposed triangular element.

The results from the examples in Chapter IV indicate that the triangular network gives temperature distributions and heat transfer rates which approach the analytical results as the size of the elements are decreased.

The temperature distribution obtained by using the triangular element in an industrial problem agrees well with the previously obtained results by the finite element method. The percentage difference in temperatures ranges from 0.006 to 1.983. These values may be considered within workable limits for general engineering practice.

Over and above the favorable accuracy associated with the proposed triangular element, its advantages in conforming to irregular boundaries, in connecting networks of different elements and in connecting fine and coarse networks are of practical importance.

The results of this investigation indicate that the proposed triangular element may be employed with confidence in the numerical solution of axisymmetric conduction problems in cylindrical coordinates.

BIBLIOGRAPHY

1. G.M. Dusinberre, Heat Transfer Calculations by Finite Differences, International Textbook Company, Scranton, 1961.

2. Walter P. Reid, "Steady State Temperature in a Triangle", Transactions of ASME Journal of Heat Transfer, August 1968, 365-366.

3. C. Lancoz, Linear Differential Operators, D. Van Nostrand Company, New York, 1961.

4. P.R. Garabedian, Partial Differential Equations, Wiley, New York, 1964.

5. E.R.G. Eckert and R.M. Drake, Heat and Mass Transfer, McGraw-Hill Book Company, Inc., New York, 1959.

6. T.R. McCalla, Introduction to Numerical Methods and Fortran Programming, John Wiley and Sons, Inc., New York, 1966.

7. V.S. Arpaci, Conduction Heat Transfer, Addison Wesley Publishing Company, Massachusetts, 1966.

8. R.L. Davis, H.D. Keith, K. Hambacker, Department of Engineering Mechanics, University of Missouri-Rolla, Personal Correspondence. April, 1971.

VITA

The author, Prafulla Chandra Mahata, was born on May 19, 1947 in Purulia, India. After his primary and higher secondary education in Purulia, India, he attended the Indian Institute of Technology, Kharagpur, India and received a Bachelor's degree in Mechanical Engineering with first class honors in June, 1969. He was a recipient of National Scholarship throughout his undergraduate studies.

He has been enrolled in the graduate school of the University of Missouri-Rolla, U.S.A. since January, 1970.

The author is a member of the National Honor Society of Phi Kappa Phi, U.S.A. and is a student member of A.S.M.E.

APPENDIX A

LENGTHS OF PERPENDICULAR BISECTORS OF A TRIANGULAR ELEMENT IN CYLINDRICAL COORDINATE SYSTEM

The lengths of the perpendicular bisectors of a triangular element must be known to use the triangular network method in two dimensional (r,z) cylindrical coordinates to solve problems of conduction. In this appendix expressions for the lengths of the perpendicular bisectors are derived in terms of the coordinates of the vertices of the triangular element.

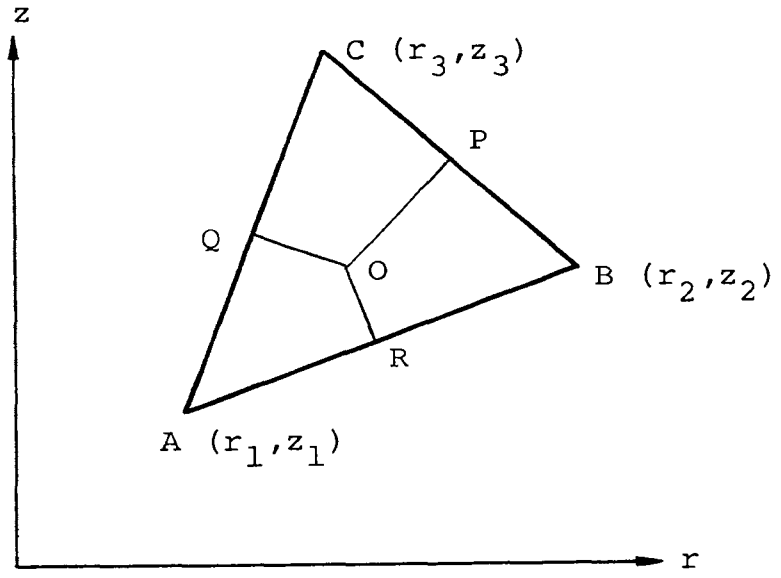

Fig. A1. A Triangular Element in Two Dimensional Cylindrical Coordinates

Triangular element with section ABC in the two dimensional cylindrical coordinate system (Fig.A1) has vertices

at (r_1,z_1), (r_2,z_2) and (r_3,z_3), respectively. OR, OP and OQ are the perpendicular bisectors. The coordinates of the mid points R, P and Q are

$$[(r_1+r_2)/2,\ (z_1+z_2)/2],\ [(r_2+r_3)/2,\ (z_2+z_3)/2]$$

and $[(r_3+r_1)/2,\ (z_3+z_1)/2]$, respectively. The equations of the lines OR, OP and OQ, passing through the mid points of and perpendicular to AB, BC and CA are

$$z = [-(r_1-r_2)/(z_1-z_2)r+[(r_1^2+z_1^2)-(r_2^2+z_2^2)]/[2(z_1-z_2)],$$

$$z = [-(r_2-r_3)/(z_2-z_3)]r+[(r_2^2+z_2^2)-(r_3^2+z_3^2)]/[2(z_2-z_3)],$$

$$z = [-(r_3-r_1)/(z_3-z_1)]r+[(r_3^2+z_3^2)-(r_1^2+z_1^2)]/[2(z_3-z_1)]. \qquad (A-1)$$

The central point O is the point of intersection of the three perpendicular bisectors and its coordinates (r_O, z_O) are given by

$$r_O = [z_1((r_2^2+z_2^2)-(r_3^2+z_3^2))+z_2((r_3^2+z_3^2)-(r_1^2-z_1^2)) + z_3((r_1^2+z_1^2)-(r_2^2+z_2^2))]/[2(z_1(r_2-r_3) + z_2(r_3-r_1)+z_3(r_1-r_2)],$$

$$z_O = [-(r_1-r_2)/(z_1-z_2)]r_O + [(r_1^2+z_1^2)-(r_2^2+z_2^2)]/[2(z_1-z_2)],$$

when $z_1 \neq z_2$. If $z_2 \neq z_3$

$$z_o = [-(r_2-r_3)/(z_2-z_3)]r_o+[(r_2^2+z_2^2)-(r_3^2+z_3^2)]/[2(z_2-z_3)]. \quad \text{(A-2)}$$

The lengths of the perpendicular bisectors are given by

$$OR = [(r_o-(r_1+r_2)/2)^2+(z_o-(z_1+z_2)/2)^2]^{1/2},$$

$$OP = [(r_o-(r_2+r_3)/2)^2+(z_o-(z_2+z_3)/2)^2]^{1/2},$$

$$OQ = [(r_o-(r_3+r_1)/2)^2+(z_o-(z_3+z_1)/2)^2]^{1/2}.$$

APPENDIX B

AN ALGEBRAIC APPROACH TO RELATE THE THERMAL CONDUCTANCES OF RECTANGULAR AND TRIANGULAR ELEMENTS IN CYLINDRICAL COORDINATES

Here an algebraic analysis is performed to investigate the possible equivalence of the rectangular (based on arithmetic mean area) and triangular (case 1 - with exact area) elements in cylindrical coordinates. The line of attack resembles Dusinberre's approach in the two dimensional rectangular coordinates. The results show that the exact equivalence of the rectangular and the triangular elements in the cylindrical coordinates does not exist. The numerical approach in Chapter III supports this conclusion. However, it is difficult to eliminate the possibility of equivalence. With a carefully chosen definition of thermal conductivity for the triangular elements, it may be possible to establish the proposed equivalence.

In Fig.B1, the rectangular element with section AXYZ is composed of the triangular elements with sections ABC, AXB, BYC and CZA. The perpendicular bisectors have mid-points N, L and M. The angle H made by the side AB with the assumed direction of heat transfer is arbitrary. The expressions for the geometric factors and hence for the thermal conductances for both the rectangular and the triangular elements will now be found.

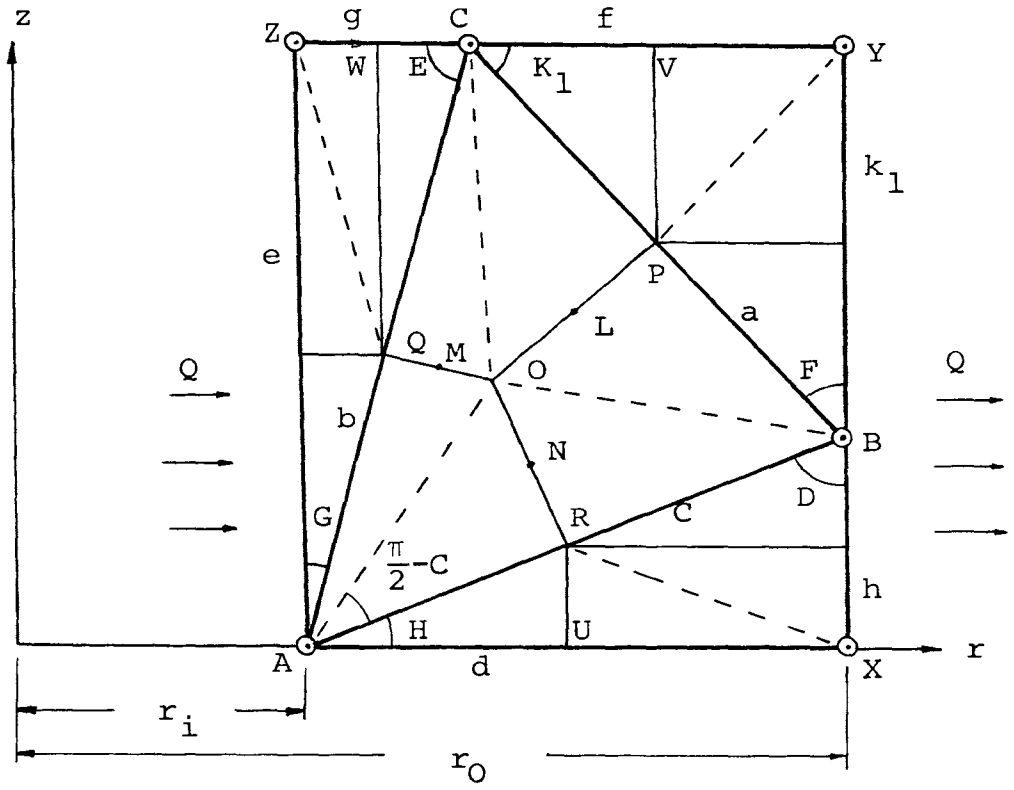

Fig.B1. A Sectional View of the Rectangular and Triangular Elements

It is expected that the geometric factor S_R for the rectangular element, defined on the basis of arithmetic mean area, has a greater possibility of yielding the proposed equivalence than that, defined on the basis of logarithmic mean area. The expression for S_R is

$$S_R = [2\pi((r_i+r_o)/2)e](r_o-r_i). \qquad (B-1)$$

Introducing $d = r_o - r_i$ in Eq. (B-1), the geometric factor and the thermal conductance can be written as

$$S_R = \pi e(2r_i+d)/d, \quad K_R = \pi ke(2r_i+d)/d, \tag{B-2}$$

where k is conductivity. For the triangular elements, the geometric factors are defined on the basis of mid-radii of the perpendicular bisectors. The geometric factors are then

$$S_{A-B} = 2\pi[(r_O+r_R)/2]OR/AB, \; S_{B-C} = 2\pi[(r_O+r_P)/2]OP/BC,$$

$$S_{C-A} = 2\pi[(r_O+r_Q)/2]OQ/CA, \; S_{A-X} = 2\pi\, r_R \cdot RU/AX,$$

$$S_{C-Y} = 2\pi r_P \cdot PV/CY, \quad S_{C-Z} = 2\pi r_Q \cdot QW/CZ. \tag{B-3}$$

The triangular elements with sections ABC, AXB, BYC and CZA are completely defined by the parameters r_i, d, e, g and h. Hence all pertinent dimensions and angles can be expressed in terms of these five independent parameters. It can be shown from geometry that

$$\angle A = \angle BOP, \quad \angle B = \angle COQ, \quad \angle C = \angle AOR, \quad \text{etc.}, \tag{B-4}$$

which leads to the trigonometric relations

$$\begin{aligned} &\text{COT C} = OR/(AB/2), \; \text{COT A} = OP/(BC/2), \\ &\text{COT B} = OQ/(CA/2), \; \text{COT D} = RU/(AX/2), \\ &\text{COT F} = PV/(CY/2), \; \text{COT G} = QW/(CZ/2), \end{aligned} \tag{B-5}$$

$$r_O = r_i + OA \cos(\pi/2 - C+H), \tag{B-6}$$

where

$$OA = c/(2 \sin C). \tag{B-7}$$

Eq. (B-6) simplifies to

$$r_o = r_i + (h/2)(\text{COT } H - \text{COT } C). \tag{B-8}$$

The radii of the points R, P and Q are

$$r_R = r_i + d/2, \quad r_P = r_i + d/2 + g/2, \quad r_Q = r_i + g/2. \tag{B-9}$$

When Eqs. (B-5), (B-8) and (B-9) are introduced into Eqs. (B-3), the geometric factors can be expressed as

$$S_{A-B} = \pi \text{ COT } C[r_i + d/4 + (h/4)(\text{COT } H - \text{COT } C)],$$

$$S_{B-C} = \pi \text{ COT } A[r_i + d/4 + g/4 + (h/4)(\text{COT } H - \text{COT } C)],$$

$$S_{C-A} = \pi \text{ COT } B[r_i + g/4 + (h/4)(\text{COT } H - \text{COT } C)],$$

$$S_{A-X} = \pi \text{ COT } D[r_i + d/2], \quad S_{C-Y} = \pi \text{ COT } F[r_i + d/2 + g/2],$$

$$S_{C-Z} = \pi \text{ COT } G[r_i + g/2). \tag{B-10}$$

The cotangents in the above equations may be expressed in terms of d, e, g and h by using the trigonometric relations [1],

$$\begin{aligned} &\text{COT } A \text{ COT } B + \text{COT } B \text{ COT } C + \text{COT } C \text{ COT } A = 1, \\ &\text{COT } K_1 \text{ COT } C + \text{COT } C \text{ COT } E + \text{COT } E \text{ COT } K_1 = 1, \\ &\text{COT } F \text{ COT } B + \text{COT } B \text{ COT } D + \text{COT } D \text{ COT } F = 1, \\ &\text{COT } G + \text{COT } A + \text{COT } H = \text{COT } G \text{ COT } A \text{ COT } H. \end{aligned} \tag{B-10}$$

Representing the cotangents of the angles by the angles for simplicity, the Eqs. (B-10) can be rewritten as

$$A\cdot B+B\cdot C+C\cdot A = 1,\ K_1\cdot C+C\cdot E+E\cdot K_1 = 1,$$
$$F\cdot B+B\cdot D+D\cdot F = 1,\ G+A+H = G\ A\ H\ . \qquad \text{(B-11)}$$

With the relations

$$D = 1/H,\ F = 1/K_1, \qquad \text{(B-12)}$$

the expressions for A, B and C are obtained from Eqs. (B-11) as

$$A = (G+H)/(GH-1),\ B = (HK_1-1)/(H+K_1),$$
$$C = (1-EK_1)/(K_1+E). \qquad \text{(B-13)}$$

Using the trigonometric relations

$$\text{COT } D = h/d,\ \text{COT } E = g/e,\ \text{COT } F = (e-h)/(d-g),$$
$$\text{COT } G = e/g,\ \text{COT } H = d/h,\ \text{COT } K_1 = (d-g)/(e-h), \qquad \text{(B-14)}$$

the Eqs. (B-13) become

$$\text{COT } A = (dg+eh)/(de-gh),\ \text{COT } B = (d^2+h^2-dg-eh)/$$
$$(de-gh), \qquad \text{(B-15)}$$
$$\text{COT } C = (e^2+g^2-dg-eh)/(de-gh).$$

Inserting the values of the cotangents from Eqs. (B-14) and (B-15) into Eqs. (B-10), all the geometric factors are expressed in terms of r_i, d, e, g and h as

$$S_{A-B} = \pi[(e^2+g^2-dg-eh)/(de-gh)][r_i+d/4+(h/4)$$
$$((e(d^2+h^2)-h(e^2+g^2))/(h(de-gh)))],$$

$$S_{B-C} = \pi[(dg+eh)/(de-gh)][r_i+d/4+g/4+(h/4)$$
$$((e(d^2+h^2)-h(e^2+g^2))/(h(de-gh)))],$$

$$S_{C-A} = \pi[(d^2+h^2-dg-eh)/(de-gh)][r_i+g/4+(h/4)$$
$$((e(d^2+h^2)-h(e^2+g^2))/(h(de-gh)))]$$

$$S_{A-X} = \pi[h/d][r_i+d/2],$$

$$S_{C-Y} = \pi[(e-h)/(d-g)][r_i+d/2+g/2],$$

$$S_{C-Z} = \pi[e/g][r_i+g/2]. \qquad \text{(B-16)}$$

The resultant conductance K_T of the triangular elements in the direction of heat transfer can be obtained by the electrical analogy as

$$K_T = k[(S_{C-A}+S_{C-Z})(S_{B-C}+S_{C-Y})/(S_{C-A}+S_{C-Z}+S_{B-C}+$$
$$S_{C-Y})+S_{A-B}+S_{A-X}]. \qquad \text{(B-17)}$$

The individual geometric factors, obtained from Eqs. (B-16) were substituted in Eq. (B-17) to get K_T in terms of r_i, d, e, g and h. The expression for K_T was then simplified. This simplification showed that the exact equivalence did not exist.